



# **NAVAL POSTGRADUATE SCHOOL**

**MONTEREY, CALIFORNIA**

## **THESIS**

**INFLUENCE OF THE ANTARCTIC CIRCUMPOLAR  
CURRENT ON THE ATLANTIC MERIDIONAL  
CIRCULATION**

by

David J. Widener

March 2009

Thesis Advisor:  
Second Reader:

Timour Radko  
Jeffrey Haferman

**Approved for public release; distribution is unlimited**

THIS PAGE INTENTIONALLY LEFT BLANK

|  |   |  |  |  |
|--|---|--|--|--|
| <b>REPORT DOCUMENTATION PAGE</b>   |   |  | <i>Form Approved OMB No. 0704-0188</i>                     |  |
| Public reporting burden for this collection of information is estimated to average 1 hour per response, including the time for reviewing instruction, searching existing data sources, gathering and maintaining the data needed, and completing and reviewing the collection of information. Send comments regarding this burden estimate or any other aspect of this collection of information, including suggestions for reducing this burden, to Washington headquarters Services, Directorate for Information Operations and Reports, 1215 Jefferson Davis Highway, Suite 1204, Arlington, VA 22202-4302, and to the Office of Management and Budget, Paperwork Reduction Project (0704-0188) Washington DC 20503.  |   |  |  |  |
| <b>1. AGENCY USE ONLY (Leave blank)</b>  |   | <b>2. REPORT DATE</b><br>March 2009                            | <b>3. REPORT TYPE AND DATES COVERED</b><br>Master's Thesis |  |
| <b>4. TITLE AND SUBTITLE</b> Influence of the Antarctic Circumpolar Current on the Atlantic Meridional Circulation   |   |  | <b>5. FUNDING NUMBERS</b>                                  |  |
| <b>6. AUTHOR(S)</b> David J. Widener   |   |  |  |  |
| <b>7. PERFORMING ORGANIZATION NAME(S) AND ADDRESS(ES)</b><br>Naval Postgraduate School<br>Monterey, CA 93943-5000  |   |  | <b>8. PERFORMING ORGANIZATION REPORT NUMBER</b>            |  |
| <b>9. SPONSORING /MONITORING AGENCY NAME(S) AND ADDRESS(ES)</b><br>N/A   |   |  | <b>10. SPONSORING/MONITORING AGENCY REPORT NUMBER</b>      |  |
| <b>11. SUPPLEMENTARY NOTES</b> The views expressed in this thesis are those of the author and do not reflect the official policy or position of the Department of Defense or the U.S. Government.  |   |  |  |  |
| <b>12a. DISTRIBUTION / AVAILABILITY STATEMENT</b><br>Approved for public release; distribution is unlimited  |   |  | <b>12b. DISTRIBUTION CODE</b>                              |  |
| <b>13. ABSTRACT (maximum 200 words)</b><br><br><p>The physics of the Meridional Overturning Circulation and inter-hemispheric heat transport is explored with an emphasis on the upper and central ocean using a general ocean circulation model. The ability of the Antarctic Circumpolar Current, bathymetry, and surface temperature and wind stresses to influence the MOC and inter-hemispheric heat transport is considered. All experiments are based on an idealized model of intermediate complexity with analysis focused on the interplay between the surface heat fluxes, geometry, and the meridional transport of heat and volume.</p> <p>The ACC is found to have an effect comparable in magnitude to that of the mechanical and thermodynamic surface forcing upon meridional circulation and inter-hemispheric heat transport. Basin geometry also plays a comparatively minor role in the inter-hemispheric transports but is essential in creating a realistic ACC by removing some of the momentum imparted by surface wind stresses.</p> <p>The combination of the ACC and asymmetric surface forcing results in values of inter-hemispheric transport which are comparable to actual values. This agreement suggests that previous emphasis on deep overturning in the ocean basins and small-scale mixing as a dominant factor in the driving force behind the MOC's strength and maintenance should be reconsidered, with greater emphasis being placed on studying the roles of the upper and central ocean.</p> |   |  |  |  |
| <b>14. SUBJECT TERMS</b> meridional overturning circulation, MOC, Antarctic Circumpolar Current, ACC, thermohaline circulation   |   |  | <b>15. NUMBER OF PAGES</b><br>65                           |  |
|  |   |  | <b>16. PRICE CODE</b>                                      |  |
| <b>17. SECURITY CLASSIFICATION OF REPORT</b><br>Unclassified   | <b>18. SECURITY CLASSIFICATION OF THIS PAGE</b><br>Unclassified | <b>19. SECURITY CLASSIFICATION OF ABSTRACT</b><br>Unclassified | <b>20. LIMITATION OF ABSTRACT</b><br>UU                    |  |

THIS PAGE INTENTIONALLY LEFT BLANK

**Authorized for public release; distribution is unlimited**

**INFLUENCE OF THE ANTARCTIC CIRCUMPOLAR CURRENT ON THE  
ATLANTIC MERIDIONAL CIRCULATION**

David J. Widener  
Lieutenant, United States Navy  
B.A., University of Washington, 2002

Submitted in partial fulfillment of the  
requirements for the degree of

**MASTER OF SCIENCE IN PHYSICAL OCEANOGRAPHY**

from the

**NAVAL POSTGRADUATE SCHOOL  
March 2009**

Author: David J. Widener

Approved by: Timour Radko  
Thesis Advisor

Jeffrey Haferman  
Second Reader

Jeff Paduan  
Chairman, Department of Oceanography

THIS PAGE INTENTIONALLY LEFT BLANK

## **ABSTRACT**

The physics of the Meridional Overturning Circulation and inter-hemispheric heat transport is explored with an emphasis on the upper and central ocean using a general ocean circulation model. The ability of the Antarctic Circumpolar Current, bathymetry, and surface temperature and wind stresses to influence the MOC and inter-hemispheric heat transport is considered. All experiments are based on an idealized model of intermediate complexity with analysis focused on the interplay between the surface heat fluxes, geometry, and the meridional transport of heat and volume.

The ACC is found to have an effect comparable in magnitude to that of the mechanical and thermodynamic surface forcing upon meridional circulation and inter-hemispheric heat transport. Basin geometry also plays a comparatively minor role in the inter-hemispheric transports but is essential in creating a realistic ACC by removing some of the momentum imparted by surface wind stresses.

The combination of the ACC and asymmetric surface forcing results in values of inter-hemispheric transport which are comparable to actual values. This agreement suggests that previous emphasis on deep overturning in the ocean basins and small-scale mixing as a dominant factor in the driving force behind the MOC's strength and maintenance should be reconsidered, with greater emphasis being placed on studying the roles of the upper and central ocean.

THIS PAGE INTENTIONALLY LEFT BLANK



# TABLE OF CONTENTS

|             |  |           |
|-------------|--|-----------|
| <b>I.</b>   | <b>INTRODUCTION .....</b>  | <b>1</b>  |
| <b>A.</b>   | <b>BACKGROUND.....</b>   | <b>1</b>  |
| <b>B.</b>   | <b>MERIDIONAL OVERTURNING CIRCULATION .....</b>  | <b>3</b>  |
| <b>C.</b>   | <b>THE IMPORTANCE OF ASYMMETRY .....</b>   | <b>4</b>  |
| <b>D.</b>   | <b>THE ANTARCTIC CIRCUMPOLAR CURRENT .....</b>   | <b>5</b>  |
| <b>E.</b>   | <b>MECHANISMS OF INTERACTION BETWEEN THE MOC AND<br/>ACC .....</b>                                 | <b>6</b>  |
|             | <b>1. Eddy-mixing.....</b>   | <b>7</b>  |
|             | <b>2. Northern Excursion of ACC .....</b>  | <b>7</b>  |
| <b>F.</b>   | <b>OBJECTIVES .....</b>  | <b>8</b>  |
| <b>II.</b>  | <b>MODEL DESCRIPTION .....</b>   | <b>9</b>  |
| <b>A.</b>   | <b>THE MODEL.....</b>  | <b>9</b>  |
| <b>B.</b>   | <b>CONFIGURATION .....</b>   | <b>9</b>  |
|             | <b>1. Idealized Basin.....</b>   | <b>10</b> |
|             | <b>2. Addition of the ACC .....</b>  | <b>10</b> |
|             | <b>3. Wind Stress .....</b>  | <b>10</b> |
|             | <b>4. Sea Surface Temperature .....</b>  | <b>12</b> |
| <b>III.</b> | <b>MODEL RUNS.....</b>   | <b>15</b> |
| <b>A.</b>   | <b>STRAIGHT ACC .....</b>  | <b>15</b> |
| <b>B.</b>   | <b>ASYMMETRIC BATHYMETRY.....</b>  | <b>20</b> |
| <b>C.</b>   | <b>SYMMETRIC BATHYMETRY WITH SYMMETRIC FORCING.....</b>  | <b>22</b> |
| <b>D.</b>   | <b>SYMMETRIC BATHYMETRY WITH ASYMMETRIC FORCING.....</b>   | <b>24</b> |
| <b>E.</b>   | <b>TWO-BASIN EXPERIMENT WITH SYMMETRIC<br/>BATHYMETRY AND FORCING .....</b>                        | <b>26</b> |
| <b>IV.</b>  | <b>COMPARISON OF THE NUMERICAL EXPERIMENTS .....</b>   | <b>29</b> |
| <b>A.</b>   | <b>ELEMENTS OF THE DIAGNOSTIC MODEL.....</b>   | <b>29</b> |
|             | <b>1. Volume Transport.....</b>  | <b>29</b> |
|             | <b>2. Heat Transport.....</b>  | <b>30</b> |
| <b>B.</b>   | <b>PATTERNS OF THE HEAT AND VOLUME TRANSPORT AS A<br/>FUNCTION OF FORCING AND GEOMETRY .....</b>   | <b>31</b> |
|             | <b>1. Inter-hemispheric Volume Transport .....</b>   | <b>31</b> |
|             | <b>2. Inter-hemispheric Heat Transport.....</b>  | <b>34</b> |
| <b>C.</b>   | <b>MAGNITUDE OF THE INTER-HEMISPHERIC TRANSPORT AS<br/>A FUNCTION OF FORCING AND GEOMETRY.....</b> | <b>37</b> |
| <b>V.</b>   | <b>DISCUSSION AND CONCLUSIONS.....</b>   | <b>43</b> |
| <b>VI.</b>  | <b>FUTURE RESEARCH .....</b>   | <b>45</b> |
| <b>A.</b>   | <b>EFFECTS OF THE RESOLVED EDDIES .....</b>  | <b>45</b> |
| <b>B.</b>   | <b>EFFECTS OF SALINITY.....</b>  | <b>45</b> |
| <b>C.</b>   | <b>REALISTIC FORCING.....</b>  | <b>45</b> |
| <b>D.</b>   | <b>GLOBAL MODEL.....</b>   | <b>45</b> |

|                                       |           |
|---------------------------------------|-----------|
| <b>LIST OF REFERENCES .....</b>       | <b>47</b> |
| <b>INITIAL DISTRIBUTION LIST.....</b> | <b>49</b> |

## LIST OF FIGURES

|            |  |    |
|------------|--|----|
| Figure 1.  | The Ocean Conveyor Belt (from Kuhlbrodt et al., 2004) .....  | 2  |
| Figure 2.  | Thermohaline Circulation (from Wyrski, 1961) .....   | 2  |
| Figure 3.  | Two-Cell Overturning Circulation (from Edwards, 2008) .....  | 4  |
| Figure 4.  | Symmetric Basins (After Radko, 2007) .....   | 4  |
| Figure 5.  | Asymmetric Basins (From Radko, 2007) .....   | 5  |
| Figure 6.  | The Antarctic Circumpolar Current (from Olbers et al., 2004) .....                                 | 6  |
| Figure 7.  | Eddy-mixing in isopycnal layers (After Marshall and Radko, 2003) .....                             | 7  |
| Figure 8.  | Adiabatic forcing by ACC (from Marshall and Radko, 2003) .....                                     | 8  |
| Figure 9.  | Symmetric Wind Stress .....  | 11 |
| Figure 10. | Asymmetric Wind Stress .....   | 12 |
| Figure 11. | Symmetric Sea Surface Temperature .....  | 13 |
| Figure 12. | Asymmetric Sea Surface Temperature .....   | 13 |
| Figure 13. | Two-dimensional Bathymetry for the Straight ACC Model Run .....                                    | 16 |
| Figure 14. | Three-dimensional Bathymetry for the Straight ACC Model Run .....                                  | 16 |
| Figure 15. | Straight ACC Model Run at Equilibrium .....  | 17 |
| Figure 16. | Meridional Temperature-Depth Profile .....   | 17 |
| Figure 17. | Zonal Temperature-Depth Profile .....  | 18 |
| Figure 18. | Annual Mean Net Surface Heat Flux .....  | 18 |
| Figure 19. | Representative Model Net Surface Heat Flux .....   | 19 |
| Figure 20. | Sea Surface Temperature for the Straight ACC Model Run .....                                       | 19 |
| Figure 21. | Net Surface Heat Flux for the Straight ACC Model Run .....   | 20 |
| Figure 22. | Two-dimensional Asymmetric Bathymetry .....  | 21 |
| Figure 23. | Three-dimensional Asymmetric Bathymetry .....  | 21 |
| Figure 24. | Sea Surface Temperature for Asymmetric Bathymetry .....  | 22 |
| Figure 25. | Net Surface Heat Flux for Asymmetric Bathymetry .....  | 22 |
| Figure 26. | Two-dimensional Symmetric Bathymetry .....   | 23 |
| Figure 27. | Three-dimensional Symmetric Bathymetry .....   | 23 |
| Figure 28. | Sea Surface Temperature for Symmetric Bathymetry .....   | 24 |
| Figure 29. | Net Surface Heat Flux for Symmetric Bathymetry .....   | 24 |
| Figure 30. | Sea Surface Temperature for Symmetric Bathymetry and Asymmetric<br>Forcing .....                   | 25 |
| Figure 31. | Net Surface Heat Flux for Symmetric Bathymetry and Asymmetric<br>Forcing .....                     | 25 |
| Figure 32. | Two-dimensional Two-basin Bathymetry .....   | 26 |
| Figure 33. | Three-dimensional Two-basin Bathymetry .....   | 27 |
| Figure 34. | Sea Surface Temperature for Two Basins .....   | 28 |
| Figure 35. | Net Surface Heat Flux for Two Basins .....   | 28 |
| Figure 36. | Inter-hemispheric Volume Transport for Idealized Basin with Antarctic<br>Circumpolar Current ..... | 31 |
| Figure 37. | Inter-hemispheric Volume Transport for Asymmetric Bathymetry .....                                 | 32 |
| Figure 38. | Inter-hemispheric Volume Transport for Symmetric Bathymetry .....                                  | 32 |

|            |   |    |
|------------|---|----|
| Figure 39. | Inter-hemispheric Volume Transport for Symmetric Bathymetry and Asymmetric Forcing..... | 33 |
| Figure 40. | Inter-hemispheric Volume Transport for Two Basins .....                                 | 33 |
| Figure 41. | Deep Abyssal Overturning Cell (from Boccaletti et al., 2005) .....                      | 34 |
| Figure 42. | Heatfunction for the Straight ACC Model Run.....  | 35 |
| Figure 43. | Heatfunction for the Asymmetric Bathymetry Model Run .....                              | 35 |
| Figure 44. | Heatfunction for the Symmetric Bathymetry Model Run.....                                | 36 |
| Figure 45. | Heatfunction for the Symmetric Bathymetry with Asymmetric Forcing Model Run .....       | 36 |
| Figure 46. | Heatfunction for the Two Basin Model Run .....  | 37 |
| Figure 47. | Total Heat Transport for Idealized Basin with Antarctic Circumpolar Current.....        | 39 |
| Figure 48. | Total Heat Transport for Asymmetric Bathymetry .....                                    | 40 |
| Figure 49. | Total Heat Transport for Symmetric Bathymetry .....                                     | 40 |
| Figure 50. | Total Heat Transport for Symmetric Bathymetry and Asymmetric Forcing...                 | 41 |
| Figure 51. | Total Heat Transport for Two Basins.....  | 41 |

## LIST OF TABLES

|          |                         |    |
|----------|-------------------------|----|
| Table 1. | Model Run Results ..... | 38 |
|----------|-------------------------|----|

THIS PAGE INTENTIONALLY LEFT BLANK

## ACKNOWLEDGMENTS

I would like to thank Mike Cook for all of his assistance with the programs required to perform the calculations and produce the graphs and plots contained in this thesis. Never once did he make it seem as if there was anything more important than helping the students at NPS.

I would also like to thank Dr. Jeff Haferman and his staff. Without the countless hours spent ensuring that I had the required computing resources and the programming code to run MITgcm this research could not have been performed. Dr. Haferman was miraculously able to find the time to assist me on the numerous occasions I needed it.

I especially thank Dr. Timour Radko for everything that he has done for me. I cannot emphasize enough the importance of a thesis advisor who has the knowledge and the passion for the subject, but more importantly the concern for the students. To be able to aid me throughout the process of producing this thesis while smiling every minute is a testament to his extreme patience and unparalleled guidance. I truly believe that I could not have picked a better advisor.

Finally, I would like to express my eternal gratitude for the encouragement and support of my parents and my future wife, Nicci. The constant stream of encouragement from all of them carried me through the hard times. Without their willingness to take care of the ‘home-front,’ I would have had to worry about being a responsible adult and everything that ‘real life’ entails.

Thank you all so very much.

THIS PAGE INTENTIONALLY LEFT BLANK



# **I. INTRODUCTION**

## **A. BACKGROUND**

The planet Earth is very unique in the fact that water can be found as a solid, liquid, and gas on the planet's surface. Approximately 71% of Earth's surface is covered by oceans. The existence of water in such a large amount is extremely important to the global climate because a distinct characteristic of water is its high heat-capacity, allowing the oceans to absorb a large amount of the sun's heat, which in turn provides the temperate climate necessary to support the amount and complexity of living organisms found on Earth.

The uneven heating of the Earth creates predominant regional wind patterns that, coupled with differences in thermohaline densities, drive ocean currents. These currents set up a global circulation, acting like a 'conveyor belt,' distributing the absorbed heat throughout the interior as seen in Figure 1. The warmer water reaching the higher latitudes helps temper the climate in those regions. For instance, the warm waters of the Gulf Stream spreading northeast across the Atlantic have a profound effect on the climate of Great Britain.

As the warmer, saltier water that is pushed into the higher latitudes transfers heat to the surrounding atmosphere, the water cools and becomes more dense, causing it to sink to greater depths. The sinking surface water then flows equatorward where it is reheated, becoming less dense, and subsequently returned to the surface. This cycle is known as the meridional overturning circulation (MOC) and is depicted in Figure 2.

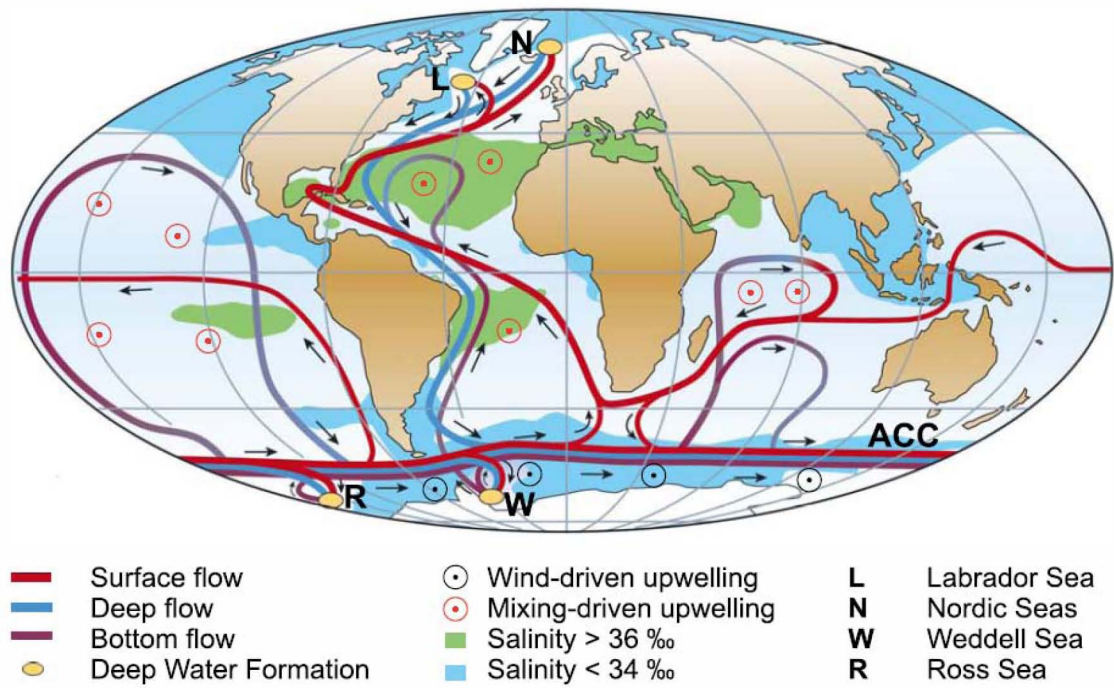


Figure 1. The Ocean Conveyor Belt (from Kuhlbrodt et al., 2004)

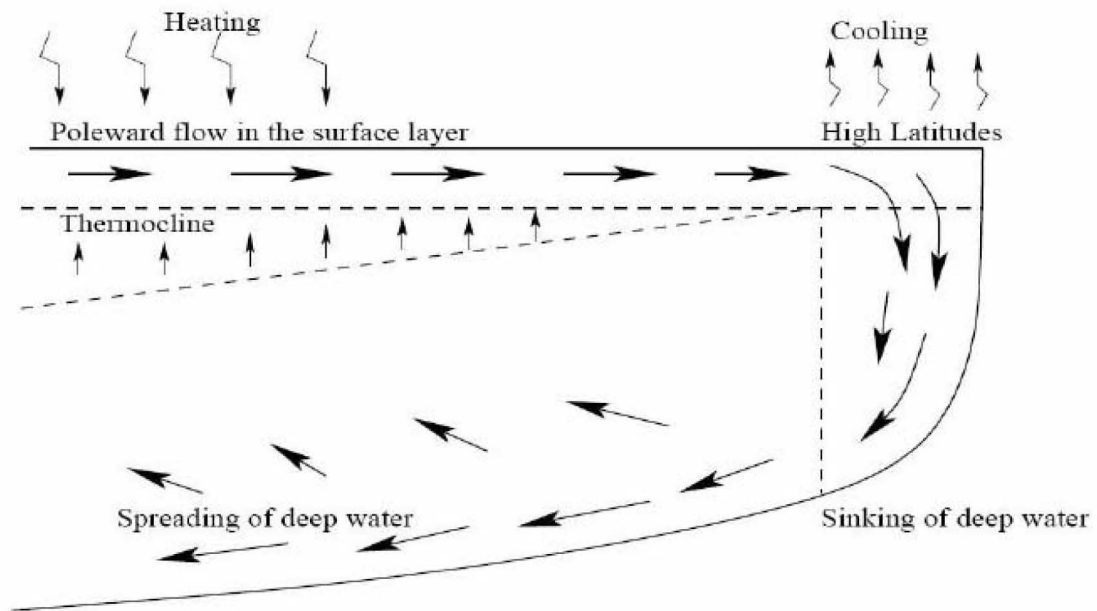


Figure 2. Thermohaline Circulation (from Wyrki, 1961)

## **B. MERIDIONAL OVERTURNING CIRCULATION**

The ocean's effect on the climate, and more recently the phenomena known as "Global Warming," has led to a great deal of interest and research in the theory of the meridional overturning circulation for the better part of the past century. One of the greatest uncertainties pertaining to the MOC is defining the mechanisms that provide its driving force.

Early research led to the opinion that interior mixing is responsible for developing and sustaining the meridional circulation (Robinson and Stommel, 1959; Munk, 1966; Welander, 1986). More recently, however, it has been argued that an unrealistic amount of vertical mixing is required to sustain such a large overturning current (Wunsch and Ferrari, 2004). Alternately, forcing due to wind stresses at the surface appears to have a significant effect on this circulation, and neglecting this input over long periods in ocean models has led to a complete shutdown of the meridional overturning (Timmermann and Goosse, 2004). Due to this discovery, considerable effort has been put forth in researching the effects of adiabatic processes on the MOC (Toggweiler and Samuels, 1998; Gnanadesikan, 1999; Marshall and Radko, 2003; Radko, 2007).

The analysis of the roles of adiabatic processes and internal mixing in driving the MOC led to the development of a two-cell model (Webb and Suginohara, 2001; Boccaletti et al., 2005). This modern theory of MOC emphasizes the differences between a deep abyssal cell and a shallow thermocline cell (see Figure 3). The abyssal cell is, for all intensive purposes, shielded from wind stress at the surface and therefore derives its potential energy for circulation through internal mixing (Wunsch and Ferrari, 2004). The shallow thermocline cell is heavily influenced by wind stress and surface heat fluxes.

This study attempts to further advance the MOC theory by clarifying the roles of mechanical and thermodynamical forcing in setting up inter-hemispheric transport. Our view is largely adiabatic, as the interior mixing is ascribed a secondary role in driving the MOC, and our focus is on the upper thermocline cell. The working hypothesis of this study is that the amount of asymmetry between the hemispheres controls the amount of meridional circulation across the equator.

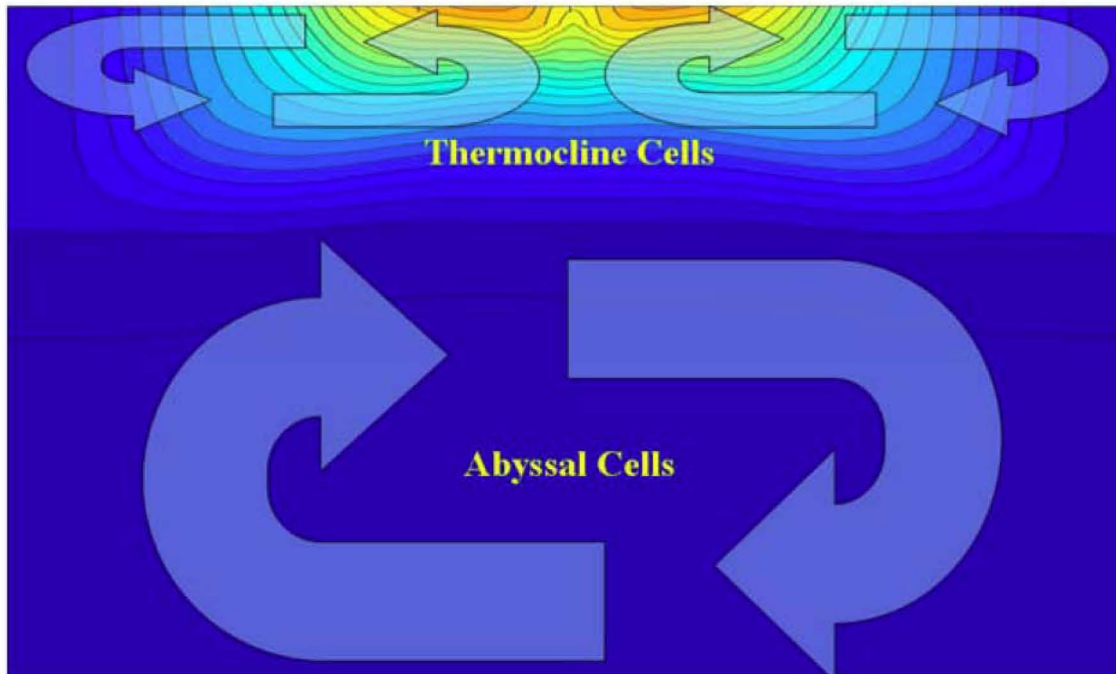


Figure 3. Two-Cell Overturning Circulation (from Edwards, 2008)

### C. THE IMPORTANCE OF ASYMMETRY

To appreciate the importance of asymmetry, imagine two hemispheres that are symmetric about the equator as in Figure 4. With a lack of asymmetry, circulation patterns in the two hemispheres are literally a mirror image of each other and therefore there can be no inter-hemispheric transport of any kind across the equator.

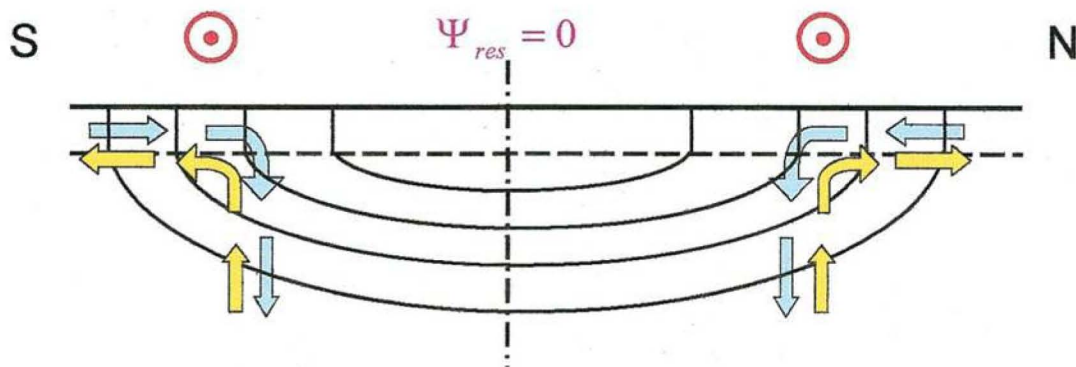


Figure 4. Symmetric Basins (After Radko, 2007)

On the other hand, if there are asymmetries between these two basins, then inter-hemispheric transport across the equator is not only possible, but also expected. For example, in Figure 5 the southern basin experiences stronger winds and higher temperatures, creating a net transport northward across the equator. This situation is representative of the modern climate.

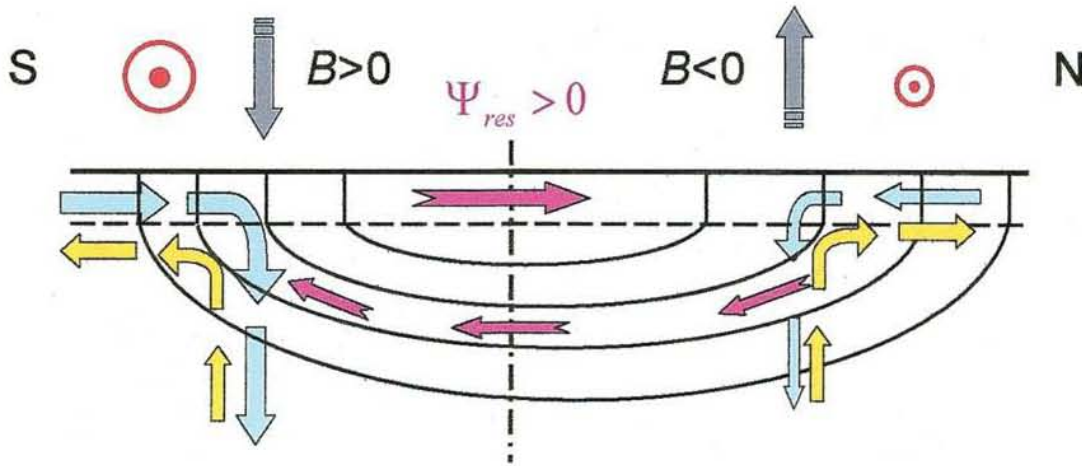


Figure 5. Asymmetric Basins (From Radko, 2007)

One striking asymmetry between the northern and southern hemispheres is the large current, known as the Antarctic Circumpolar Current (ACC), which flows around Antarctica. The purpose of this paper is to determine the effect of the ACC on the Atlantic MOC in an attempt to bring the scientific community closer to fully understanding the driving forces behind the meridional overturning circulation.

#### D. THE ANTARCTIC CIRCUMPOLAR CURRENT

The Antarctic Circumpolar Current flows around the southern portion of the Earth, encircling the entire continent of Antarctica and connecting the Atlantic, Pacific, and Indian Ocean basins. The ACC is not blocked by meridional land barriers, which allows free communication between all of the major ocean basins. Combining the lack of obstacles and a predominant westerly wind, the ACC is a very strong, wide current system with a mean volume transport of  $134 \pm 13$  Sv ( $1 \text{ Sv} = 10^6 \text{ m}^3/\text{s}$ ) through Drake's Passage (Whitworth, 1983; Whitworth and Peterson, 1985).

This intense circumpolar current does not merely follow along a single latitude in its journey around the globe (see Figure 6). Bottom topography steers the ACC northward as it leaves Drake's Passage, bringing colder Antarctic waters into the warmer northern latitudes before the current meanders back to the south as it enters the Pacific Ocean basin. The combination of this denser water closer to the equator and the momentum of the northward flow of the ACC may have a large impact on inter-hemispheric heat and volume transports.

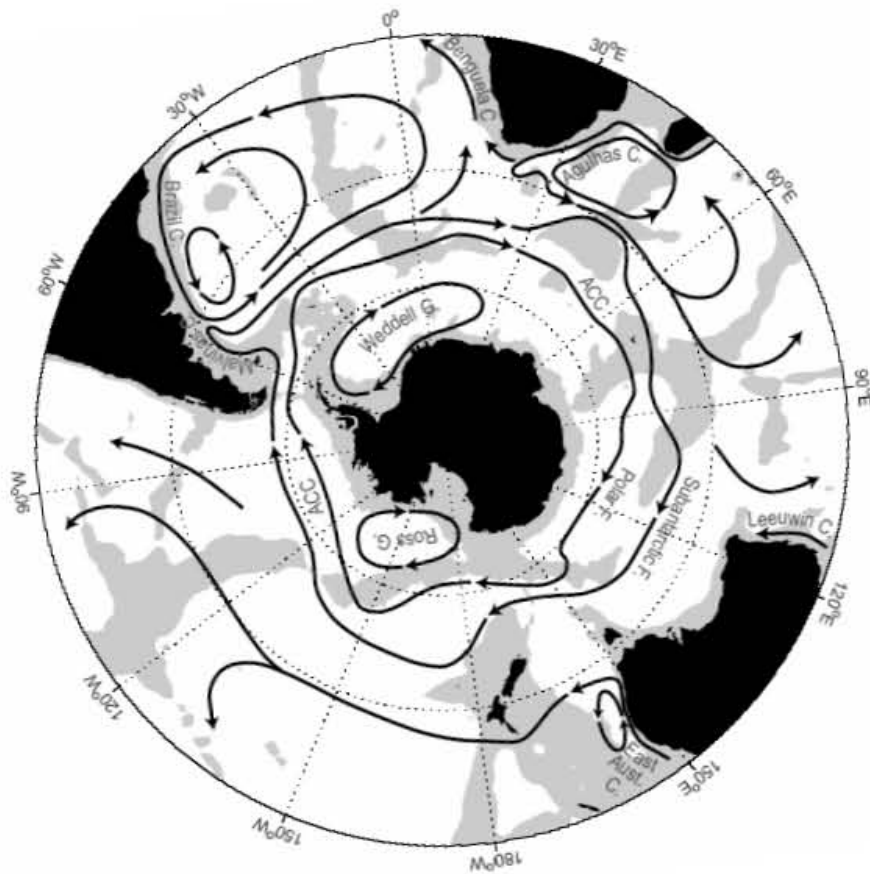


Figure 6. The Antarctic Circumpolar Current (from Olbers et al., 2004)

#### **E. MECHANISMS OF INTERACTION BETWEEN THE MOC AND ACC**

The fact that the asymmetries between the hemispheres can drive the meridional circulation is not a large stretch of the imagination. For instance, the westerly winds in the southern hemisphere drive a net northward surface current through Ekman transport.

Explaining how a west-to-east flowing current drives a north-to-south circulation, however, is a much more difficult task. There are at least two physical mechanisms that can potentially explain how the ACC could induce this overturning circulation. These mechanisms are related to eddy-mixing and the northward excursion of the ACC as it exits Drake's Passage.

## 1. Eddy-mixing

A current as strong as the ACC produces numerous eddies of varying sizes as it travels around the globe. These eddies create internal mixing within isopycnal layers, changing the geometry of the layers. Isopycnal layers tend to be much narrower near the surface and much wider in the deeper regions as shown in Figure 7. The mixing due to eddies, however, tends to homogenize the thickness of each isopycnal layer, which requires an isopycnal volume transport towards the layer outcrop. This eddy-induced transport effectively pumps the water from the deeper regions towards the surface, inducing an overturning circulation.

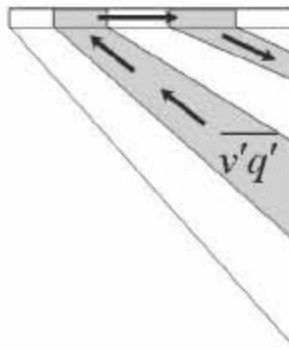


Figure 7. Eddy-mixing in isopycnal layers (After Marshall and Radko, 2003)

## 2. Northern Excursion of ACC

The foregoing two-dimensional mechanism can be further intensified by fundamentally three-dimensional effects. As previously mentioned, the ACC is diverted northward at the exit of Drake's Passage due to topographic steering. This northern excursion draws cold water from the higher latitudes equatorward where it is subjected to heating via air-sea interactions, shown in Figure 8. The positive heat fluxes cause further

equatorward motion of water in the upper diabatic layer, drawing deeper water to the surface as the upper layer flows north and thus inducing an overturning circulation in the meridional plane.

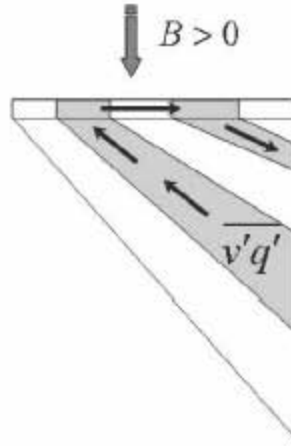


Figure 8. Adiabatic forcing by ACC (from Marshall and Radko, 2003)

## F. OBJECTIVES

The major objective of this thesis is to provide a better understanding of the influence of the Antarctic Circumpolar Current on the dynamics of meridional overturning in the upper layers of the ocean. The influence of the ACC on the MOC will be investigated by varying wind and thermal stresses as well as introducing representative bathymetry in an idealized ocean basin. Gaining an understanding of this complex system will provide more accurate models and predictions of the future climate because of the strong dependence of atmospheric conditions on the ocean circulation patterns. The ability to forecast the ocean climate also has serious implications in national security due to global warming and the potential reopening of the Northern Passage because of Arctic ice melt.



## **II. MODEL DESCRIPTION**

The influence of the ACC and other asymmetries on MOC is an intriguing idea. Independent and objective analysis is required, however, to support the theory. Numerical modeling provides the most simple and obvious method to obtain such support.

### **A. THE MODEL**

The model used in this study is the Massachusetts Institute of Technology General Circulation Model (MITgcm). MITgcm is a numerical model that can be used to study both ocean and atmospheric conditions and for both small and large-scale processes because it possesses a non-hydrostatic capability. The model employs finite volume techniques and support for the treatment of irregular geometries using orthogonal curvilinear grids and shaved cells. Sensitivity and optimization studies are also possible because tangent linear and adjoint counterparts are automatically maintained along with the forward model. MITgcm has been developed to operate efficiently on a wide variety of computational platforms. For more information about MITgcm, visit <http://mitgcm.org>.

### **B. CONFIGURATION**

The basic construction of the idealized basin and the surface forcing parameters used in this study are similar to those used in Edwards (2008) to allow for ease of comparison and discussion. It is important to note that salinity is constant throughout the basin, vertical diffusivity is kept to a minimum, and therefore all subsequent meridional overturning can be attributed solely to adiabatic and geometric effects. With MITgcm, mesoscale eddies are parameterized using the Gent-McWilliams scheme (Gent and McWilliams, 1995).

## 1. Idealized Basin

The idealized ocean basin is rectangular in shape, uses Cartesian coordinates, and spans  $60^\circ$  of longitude (6,660 km) and  $120^\circ$  of latitude (13,320 km). The box is divided into a northern and southern hemisphere of equal size. The x-direction consists of 100 grid points and the y-direction consists of 200 grid points, giving a resolution of  $0.6^\circ$  in both directions. The z-direction consists of 20 levels varying exponentially in size, from 22 m for the surface layer to 678 m for the bottom layer, for a total depth of 4005 m. This scheme allows for greater detail in the thermocline cell, which is the area of concern for this study. The resolution in the vertical direction is given for each level by the following equation:

$$\Delta Z(l) = C[\exp(\alpha l) - \exp(\alpha(l-1))] \quad (1)$$

where  $C = 112.5$  m,  $\alpha = 0.18 \text{ m}^{-1}$ , and  $l$  = the vertical level (ranging from 1 to 20).

## 2. Addition of the ACC

A critical difference between Edwards (2008) and the present study is related to the addition of the ACC. In order to represent the ACC, periodic boundary conditions were imposed to simulate a circumpolar current and a channel simulating Drake's Passage was cut out of the eastern and western boundaries. This channel spans 10 grid points in the y-direction, which is 5% of the overall length in that direction and begins 10 grid points north of the southern boundary. Drake's Passage is approximately 800 km wide, which is approximately 4.5% of the Atlantic Ocean's 18,000 km length.

## 3. Wind Stress

Wind stress is varied only in the meridional direction and contains both a symmetric and asymmetric portion (with respect to the equator). Wind stress is assumed to be zonal.

The symmetric portion of the wind stress equation is given by:

$$\tau_{sym} = \frac{3}{4} \tau_0 \left[ \frac{3}{4} \cos(5\pi\phi) - \cos(3\pi\phi) \right] \quad (2)$$

where  $\tau_0 = 0.1 \text{ Nm}^{-2}$ . The latitude term,  $\phi$ , is set such that wind stress is zero at the northern and southern edges of the computational domain.

The asymmetric portion of the equation is designed to allow a mid-latitude wind stress asymmetry without affecting the magnitude near the equator. The asymmetric portion of the wind stress equation is given by:

$$\tau_{\text{asym}} = \frac{1}{144} \tau_0 \left[ -\frac{2}{3} \sin(2\pi\phi) + \frac{11}{24} \sin(4\pi\phi) - \frac{1}{12} \sin(6\pi\phi) \right] \quad (3)$$

The combined idealized wind stress equation is:

$$\tau = \tau_{\text{sym}} - A\tau_{\text{asym}} \quad (4)$$

The coefficient of wind stress asymmetry,  $A$ , allows for easy manipulation of wind stress while performing multiple model runs. When  $A = 0$ , wind stress is symmetric about the equator and is shown in Figure 9. If  $A > 0$ , peak and mean wind stress is stronger in the northern hemisphere. Alternately, if  $A < 0$ , peak and mean wind stress is stronger in the southern hemisphere (see Figure 10).

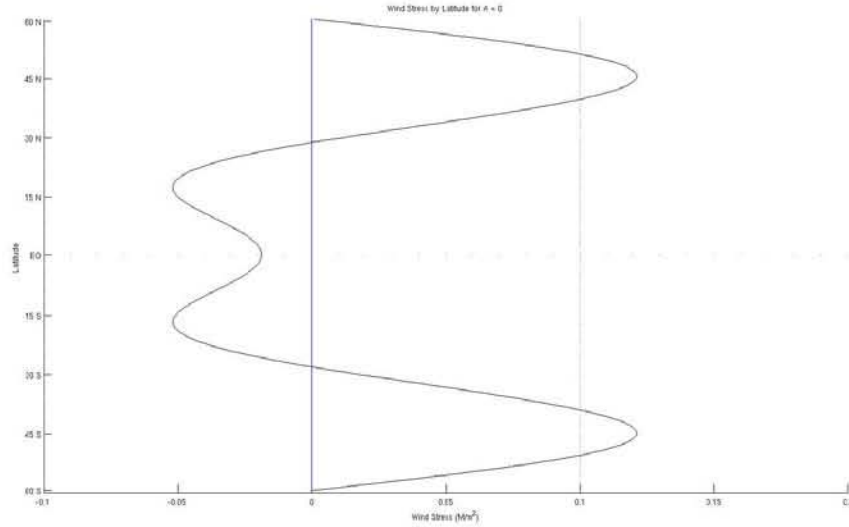


Figure 9. Symmetric Wind Stress

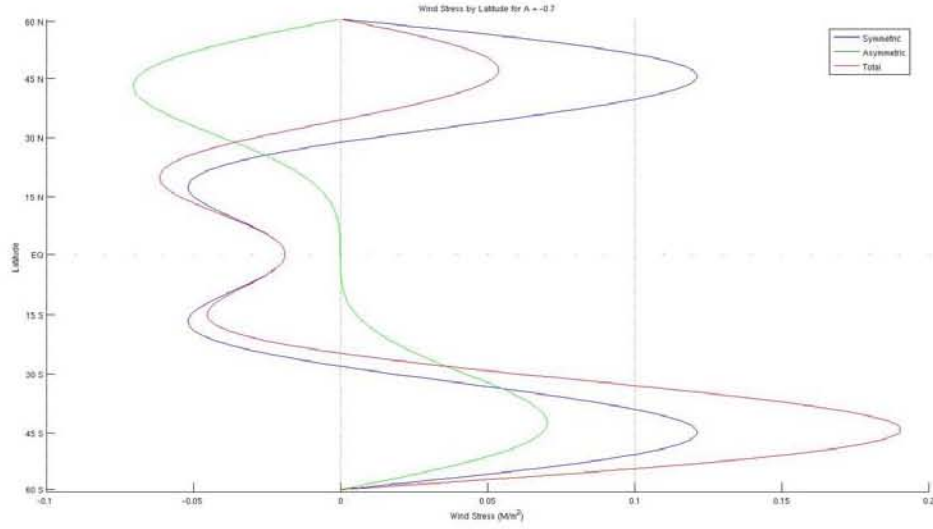


Figure 10. Asymmetric Wind Stress

#### 4. Sea Surface Temperature

The equations for temperature forcing are very similar to those of wind stress. Sea surface temperature varies only in the meridional direction and is composed of symmetric and asymmetric elements.

The symmetric portion of the sea surface temperature is given by the equation:

$$T_{sym} = T_{mid} + T_{add} \cos(2\pi\phi) \quad (5)$$

where  $T_{mid} = 13 \text{ }^{\circ}\text{C}$  and  $T_{add} = 12 \text{ }^{\circ}\text{C}$ . The latitude term,  $\phi$ , is set such that the symmetric wind equation gives a peak temperature of  $25 \text{ }^{\circ}\text{C}$  at the equator and a minimum temperature of  $1 \text{ }^{\circ}\text{C}$  at the northern and southern edges of the box.

Asymmetry of the sea surface temperature is designed such that the peak temperature remains in the equatorial band while the higher latitudes still remain around  $1 \text{ }^{\circ}\text{C}$ , and is given by the equation:

$$T_{asym} = \frac{1}{3} \sin(2\pi\phi) - \frac{1}{3} \sin(4\pi\phi) + \frac{1}{6} \sin(6\pi\phi) \quad (6)$$

The combined idealized temperature forcing equation is:

$$T = T_{sym} - BT_{asym} \quad (7)$$

The coefficient of temperature forcing asymmetry,  $B$ , allows for easy manipulation of sea surface temperature while performing multiple model runs. When  $B = 0$ , sea surface temperature is symmetric about the equator as seen in Figure 11. If  $B > 0$ , sea surface temperature is greater in the northern hemisphere. Alternately, if  $B < 0$ , sea surface temperature is greater in the southern hemisphere, shown in Figure 12.

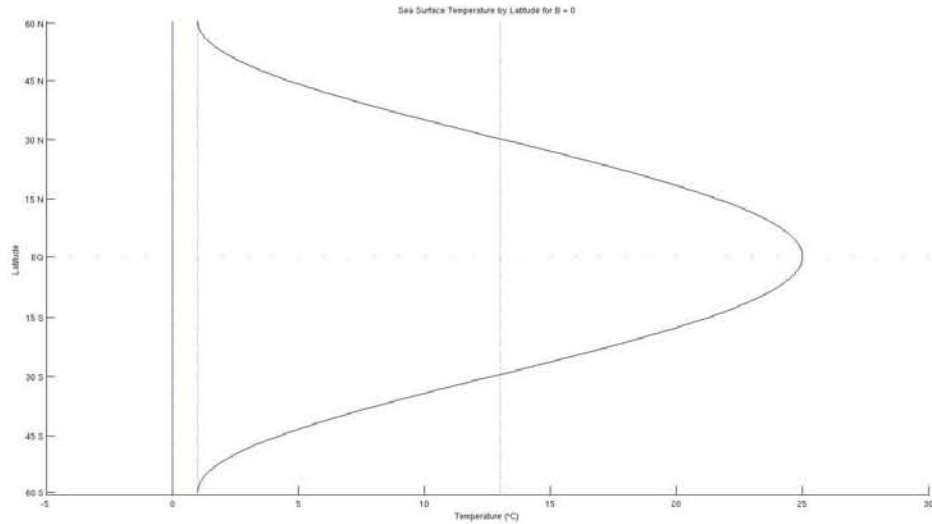


Figure 11. Symmetric Sea Surface Temperature

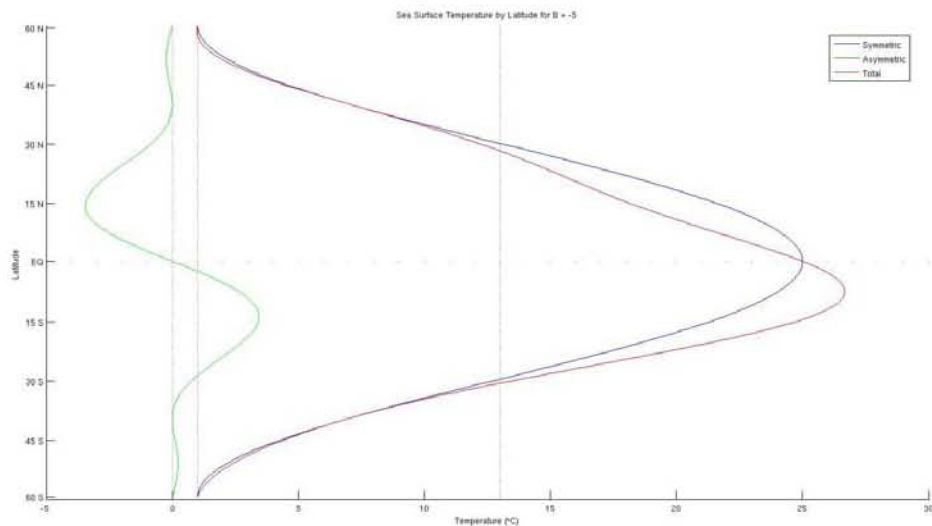


Figure 12. Asymmetric Sea Surface Temperature

THIS PAGE INTENTIONALLY LEFT BLANK

### III. MODEL RUNS

The analysis of the interaction between the ACC and MOC is based on the intercomparison of five model runs, in which forcing parameters and the basin geometry are systematically varied. In each case, the model was integrated in time until reaching the equilibrium state.

Equilibrium was determined to have been reached in each of these model runs when the inter-hemispheric heat transport reached a constant value. Heat transport is calculated using the following equation:

$$H = c_p \rho \iint_{eq} v T dz dx \quad (8)$$

It is important to note that at equilibrium, ACC and MOC volume transports still fluctuate while maintaining a constant inter-hemispheric heat transport. All of the model runs reached equilibrium at approximately 250 years.

#### A. STRAIGHT ACC

The first model run uses the simple geometry previously described. This geometry is simply a rectangular box with a channel in the southern portion of the eastern/western wall representing Drake's Passage. Figures 13 and 14 represent the bathymetry in two and three dimensions. Symmetric wind and temperature forcing were then applied and the model was exercised until equilibrium was reached (see Figure 15).

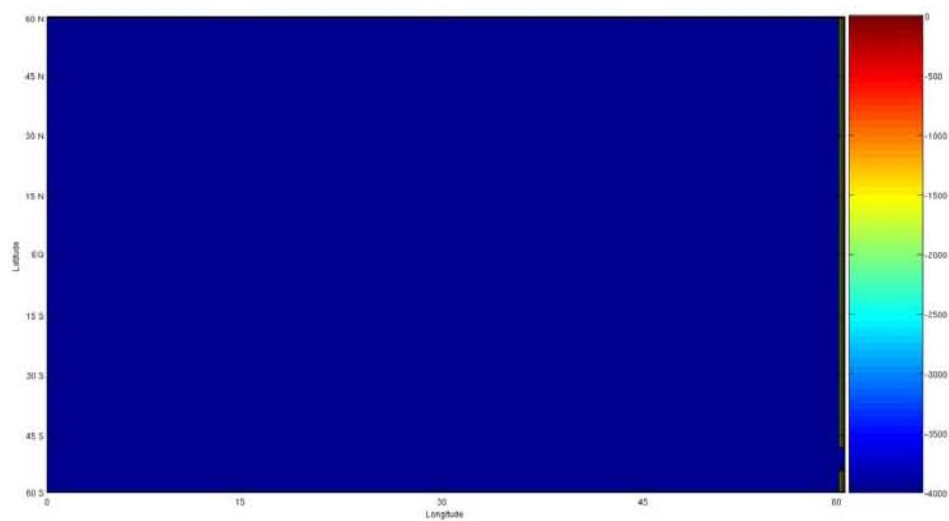


Figure 13. Two-dimensional Bathymetry for the Straight ACC Model Run

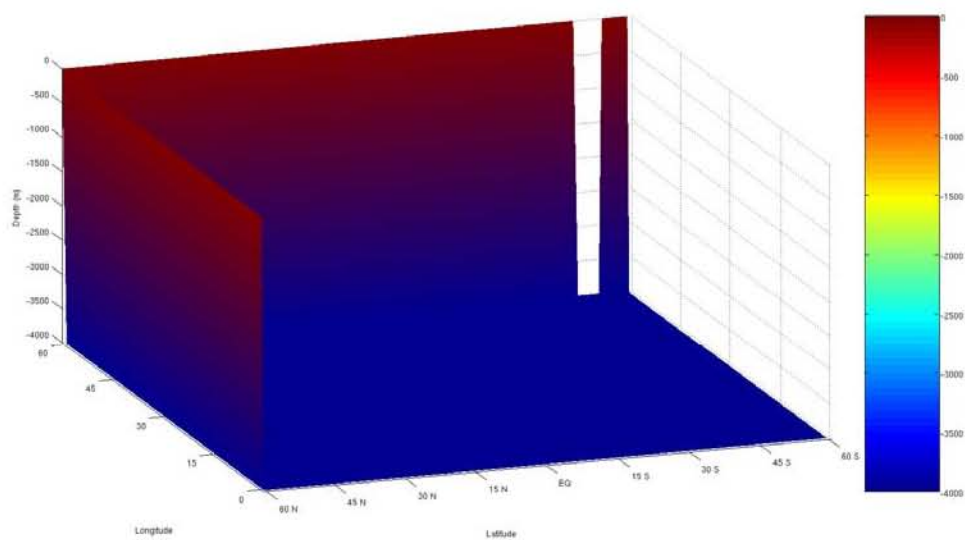


Figure 14. Three-dimensional Bathymetry for the Straight ACC Model Run



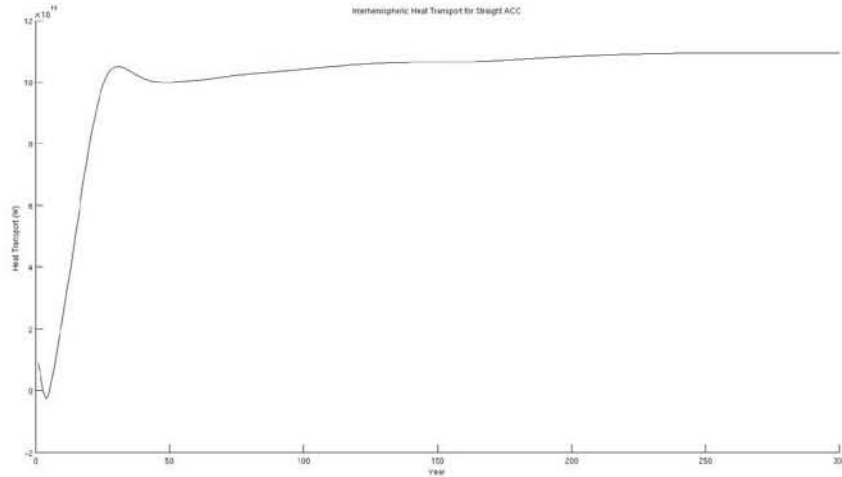


Figure 15. Straight ACC Model Run at Equilibrium

Whenever an ocean model is used in an experiment the output should always be analyzed to ensure an accurate representation of the ocean environment is created. Various cross-sections of temperature depict a virtual ocean that very closely resembles the real ocean environment. For example, Figure 16 and Figure 17 give the temperature vs. depth profile in the meridional and zonal directions, respectively. These plots show greater resolution in the thermocline layer than the abyssal layer since the focus of this research is on the thermocline layer.

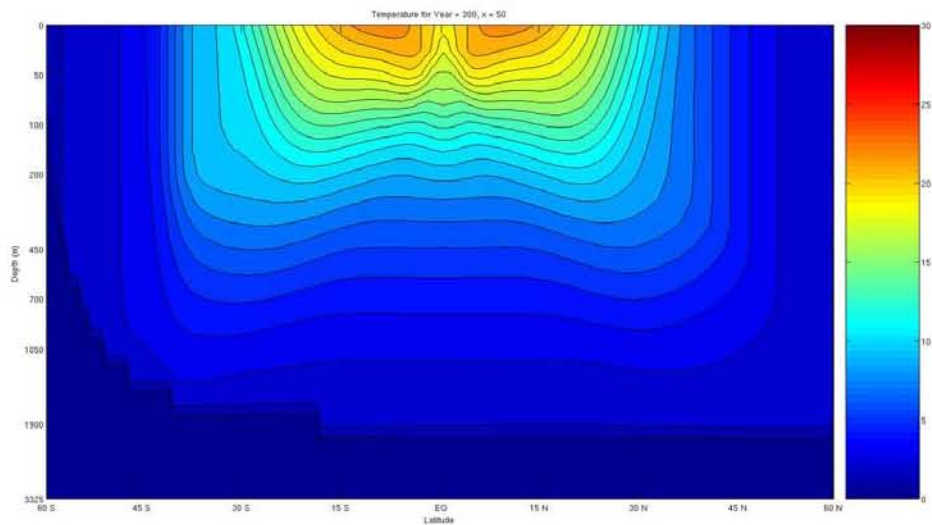


Figure 16. Meridional Temperature-Depth Profile

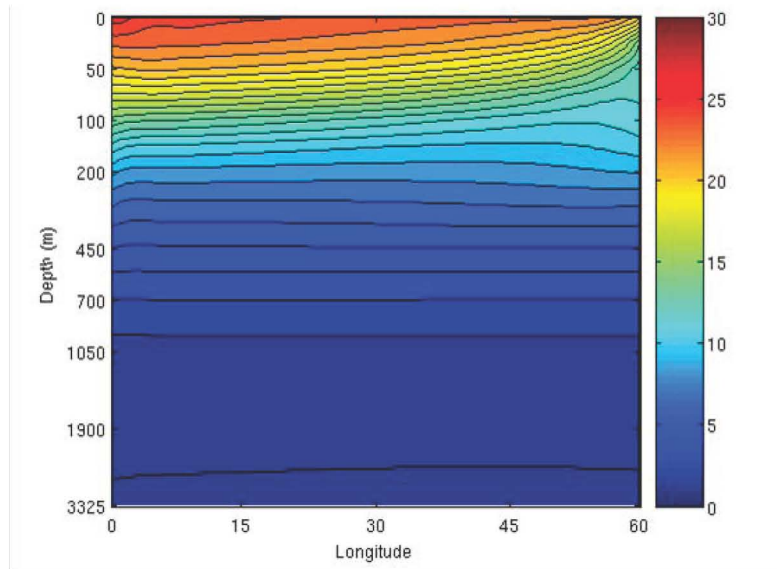


Figure 17. Zonal Temperature-Depth Profile

Heat flux at the ocean's surface is another parameter that was investigated to ensure the accuracy of the model output. Figure 18 shows the global heat flux at the ocean's surface (derived from ECMWF climatology data) and Figure 19 is a plot of the model's net surface heat flux. Note that both figures depict an area of heat escaping the ocean in the western portion of each hemisphere and the general absorption of heat in the equatorial region with a higher heat flux in the eastern segment of that equatorial band.

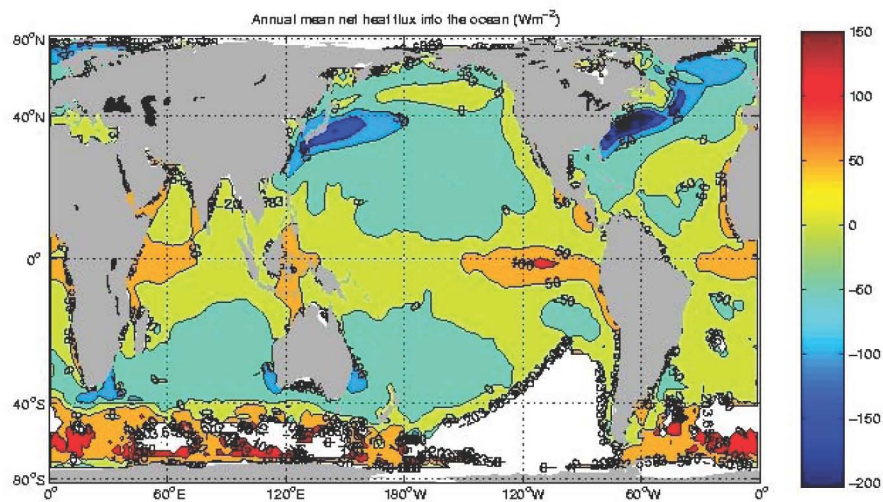


Figure 18. Annual Mean Net Surface Heat Flux

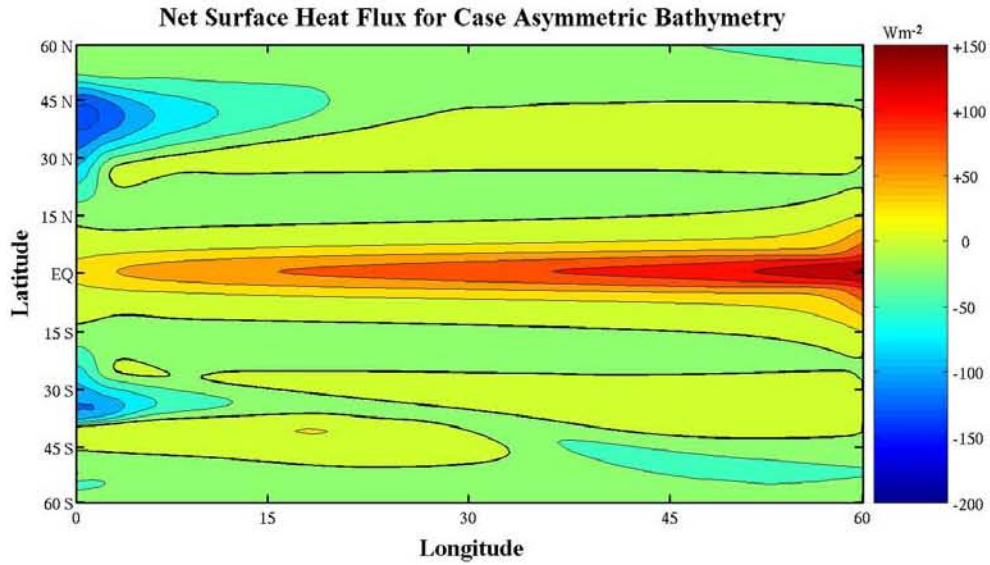


Figure 19. Representative Model Net Surface Heat Flux

The model outputs examined for each run include the sea surface temperature and net surface heat flux. Sea surface temperature averaged over the final year of the Straight ACC model run is shown in Figure 20 with warmest temperatures in red and the coldest temperatures in blue. Figure 21 represents the net surface heat flux, also averaged over the last year of the Straight ACC model run, with positive values indicating heating of the ocean and negative values representing heat transfer from the ocean to the atmosphere.

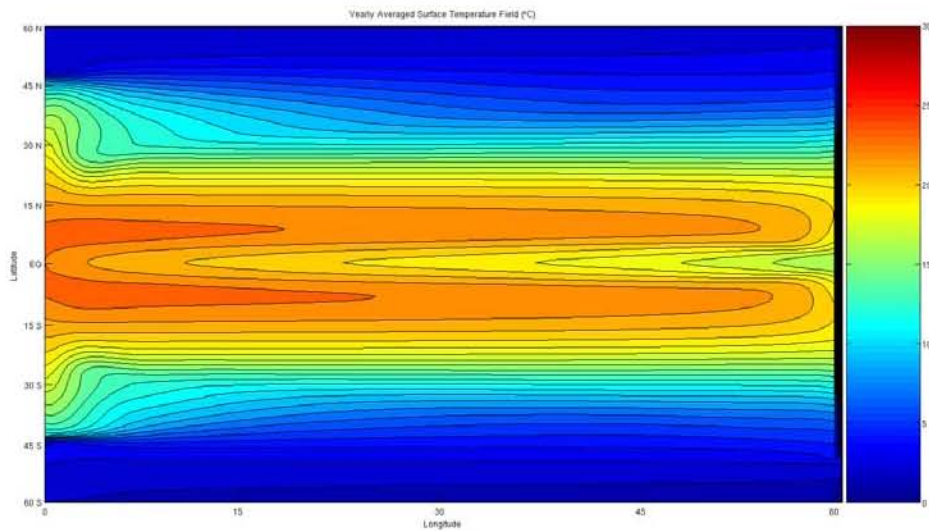


Figure 20. Sea Surface Temperature for the Straight ACC Model Run

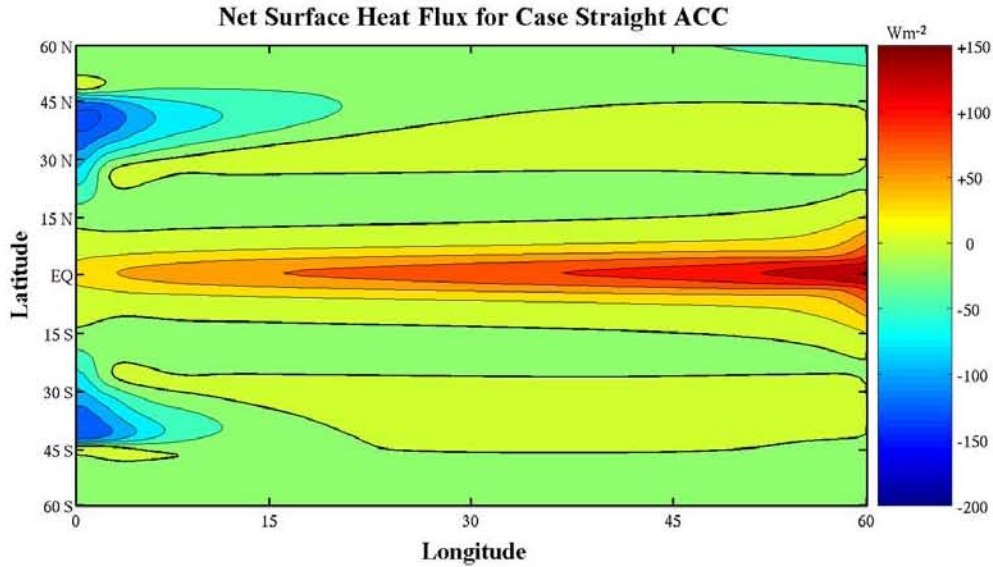


Figure 21. Net Surface Heat Flux for the Straight ACC Model Run

## B. ASYMMETRIC BATHYMETRY

The Straight ACC model run produced an unrealistically high value, approximately 360 Sv, of volume transport through Drake's Passage. Past research had led to the observation that some interaction of the ACC with bottom topography is essential in the Southern Ocean to allow bottom pressure torques to remove the momentum imparted on the current by surface winds (Munk and Palmén, 1951). Therefore, in order to bring the model into a closer agreement with observations by decreasing its volume transport, as well as steering the ACC northward (as it actually does when entering the Atlantic Ocean), asymmetric bathymetry was included. This inclusion represents a mid-Atlantic ridge as well. Figures 22 and 23 represent the two- and three-dimensional bathymetry for the asymmetric bathymetry model run. Symmetric wind and temperature forcing were then applied and the model was integrated in time until equilibrium was reached.

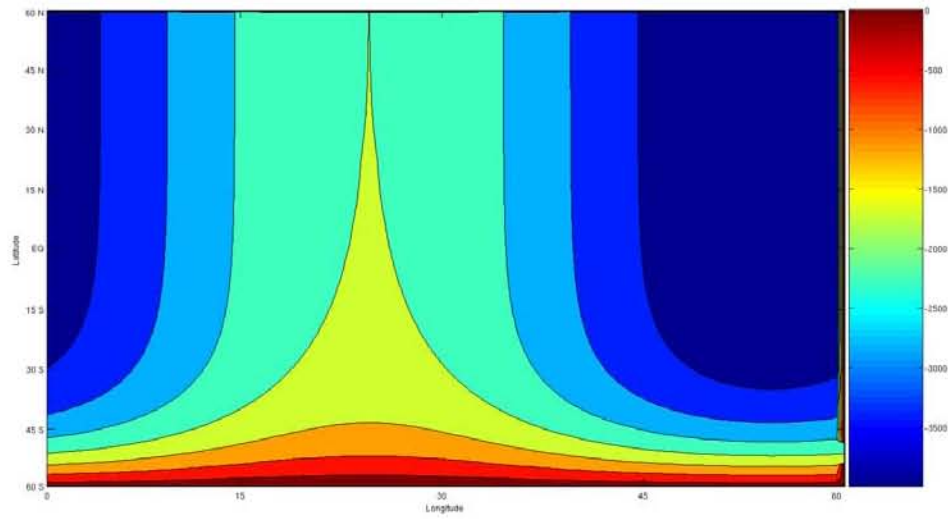


Figure 22. Two-dimensional Asymmetric Bathymetry

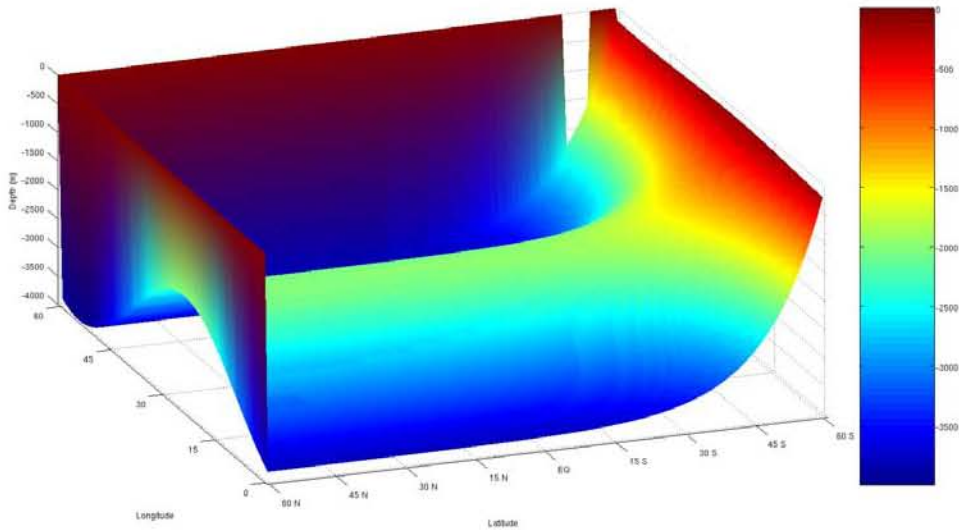


Figure 23. Three-dimensional Asymmetric Bathymetry

Figures 24 and 25 display the sea surface temperature and net surface heat flux, respectively, averaged over the last year of the asymmetric bathymetry model run. For sea surface temperature, coldest temperatures are blue with warmest temperatures in red. For net surface heat flux, positive values indicate heat transfer from the atmosphere into the ocean and negative values indicate the reverse.



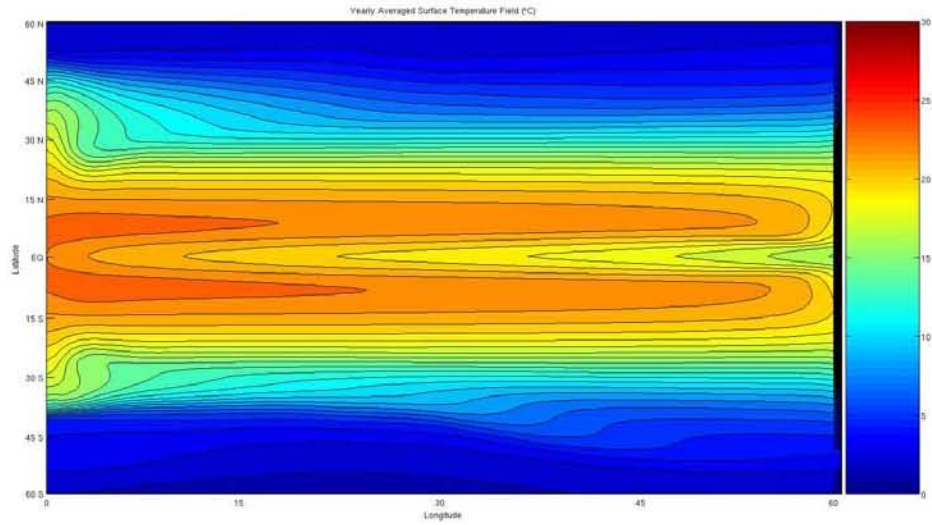


Figure 24. Sea Surface Temperature for Asymmetric Bathymetry

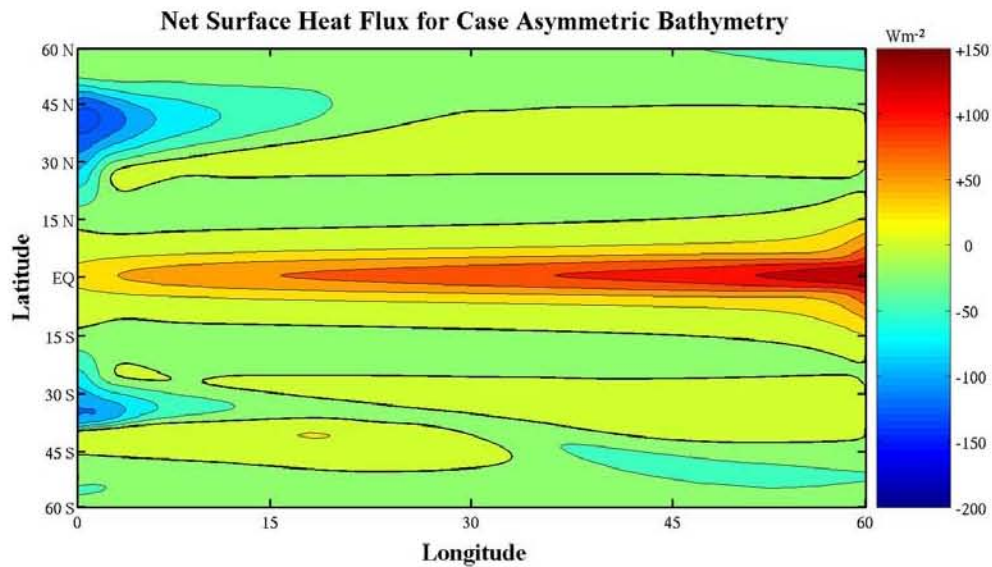


Figure 25. Net Surface Heat Flux for Asymmetric Bathymetry

### C. SYMMETRIC BATHYMETRY WITH SYMMETRIC FORCING

In order to assist in determining the effects of the ACC and those of meridional variation in bathymetry, a model using symmetric bathymetry relative to the equator was used. The symmetric bathymetry is shown in two and three dimensions in Figures 26 and 27. Symmetric wind and temperature forcing were then applied and the model was run forward in time until equilibrium was reached.

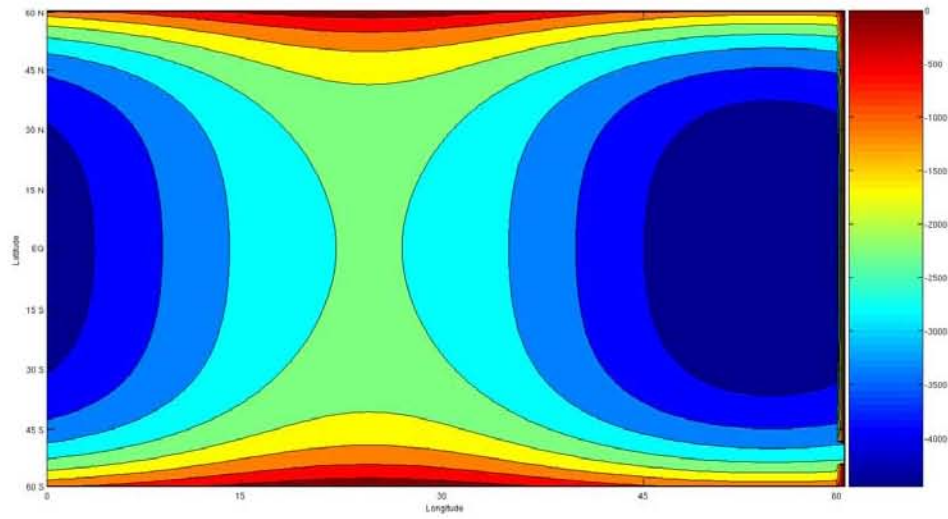


Figure 26. Two-dimensional Symmetric Bathymetry

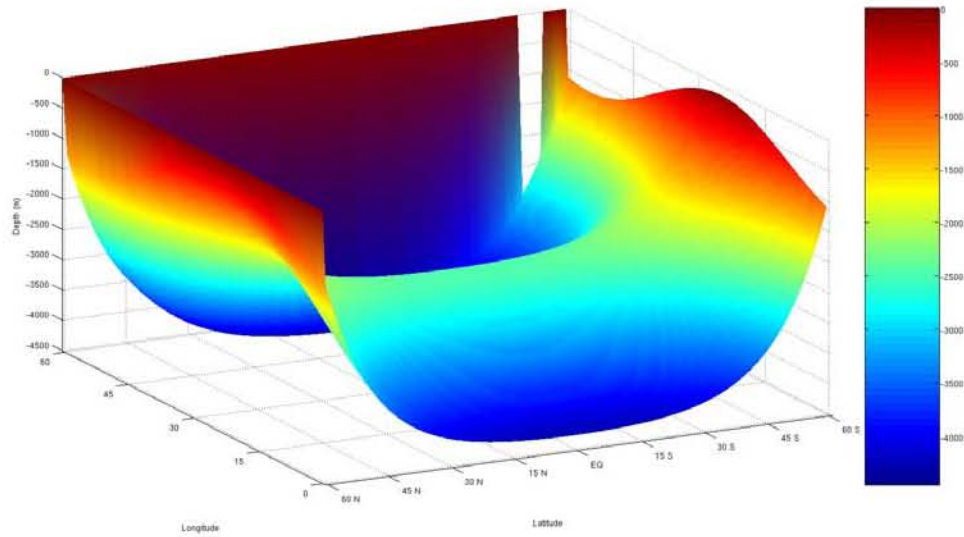


Figure 27. Three-dimensional Symmetric Bathymetry

The symmetric bathymetry model run resulted in the sea surface temperature profile shown in Figure 28 and net surface heat flux shown in Figure 29. Again, warmer sea surface temperatures are in red and colder temperatures are in blue while positive net surface heat flux values represent heating of the ocean's surface and negative values represent cooling of the ocean's surface.

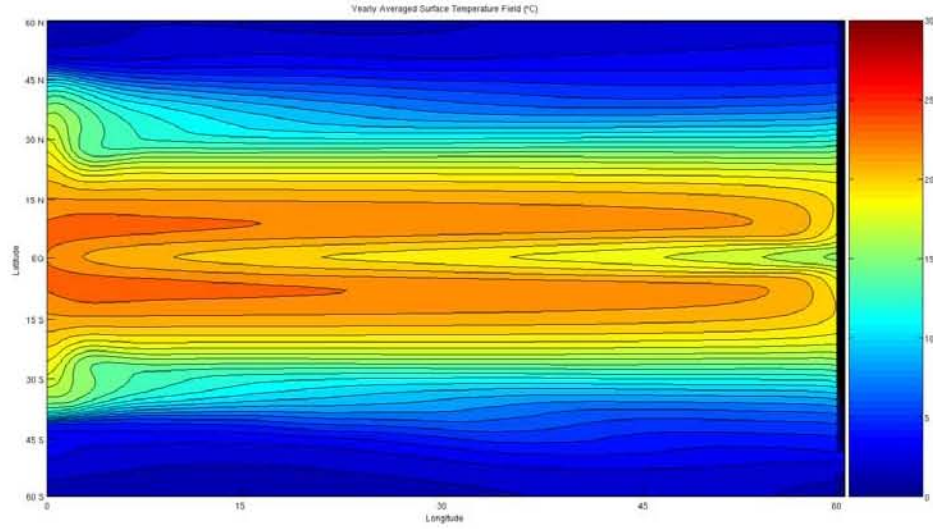


Figure 28. Sea Surface Temperature for Symmetric Bathymetry

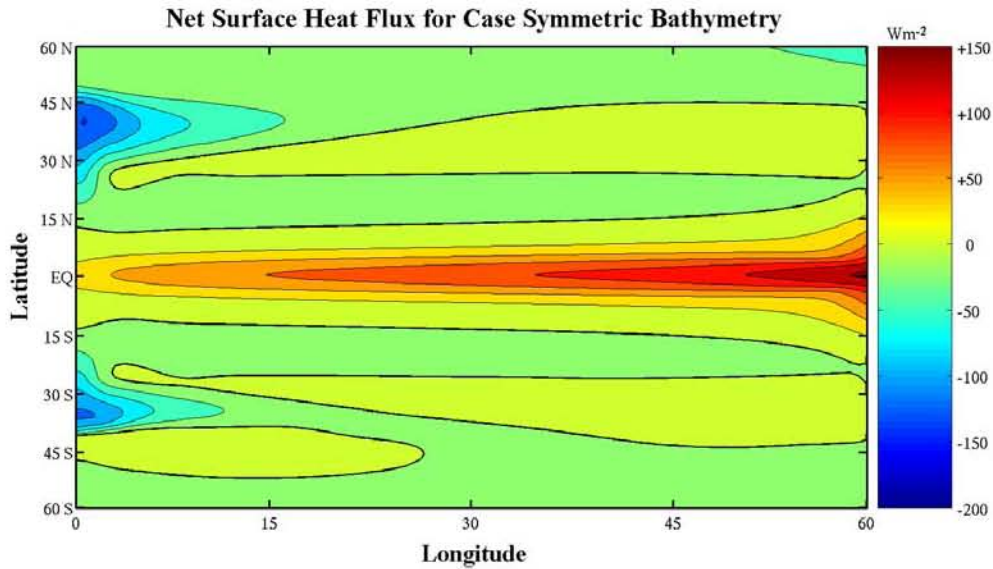


Figure 29. Net Surface Heat Flux for Symmetric Bathymetry

#### D. SYMMETRIC BATHYMETRY WITH ASYMMETRIC FORCING

The next model run used the same meridionally symmetric bathymetry from Figures 26 and 27, but asymmetric wind (Figure 10) and temperature (Figure 12) forcing representing true climatology was applied. Again, the model was run until equilibrium was reached.



Figure 30 is the resulting sea surface temperature and Figure 31 is the net surface heat flux (averaged over the last year) of the asymmetric forcing model run. Asymmetric forcing led to large asymmetries in these two figures. South of the equator, around 20°S latitude, there is a larger magnitude of negative heat flux than was seen in the other model runs. The enhanced Ekman transports, due to the stronger southern hemisphere forcing, converging in this zone may possibly be an explanation for this observation.

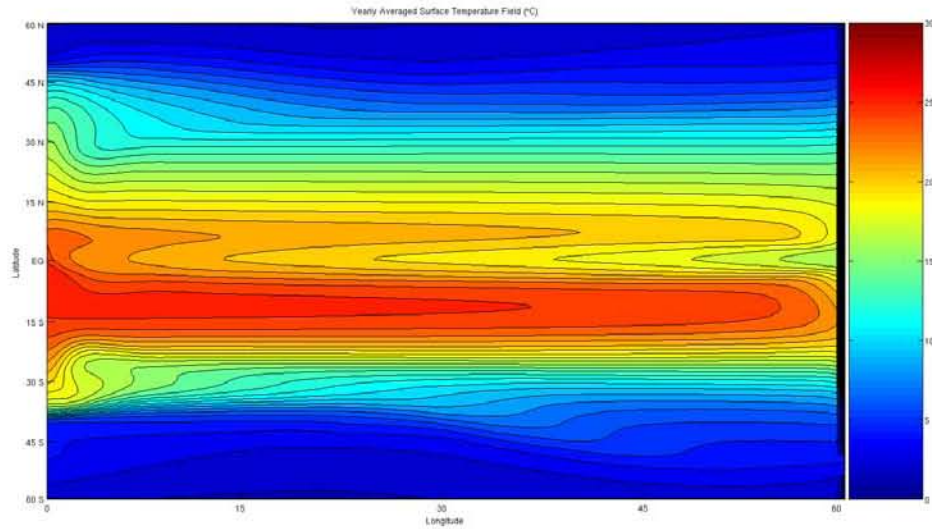


Figure 30. Sea Surface Temperature for Symmetric Bathymetry and Asymmetric Forcing

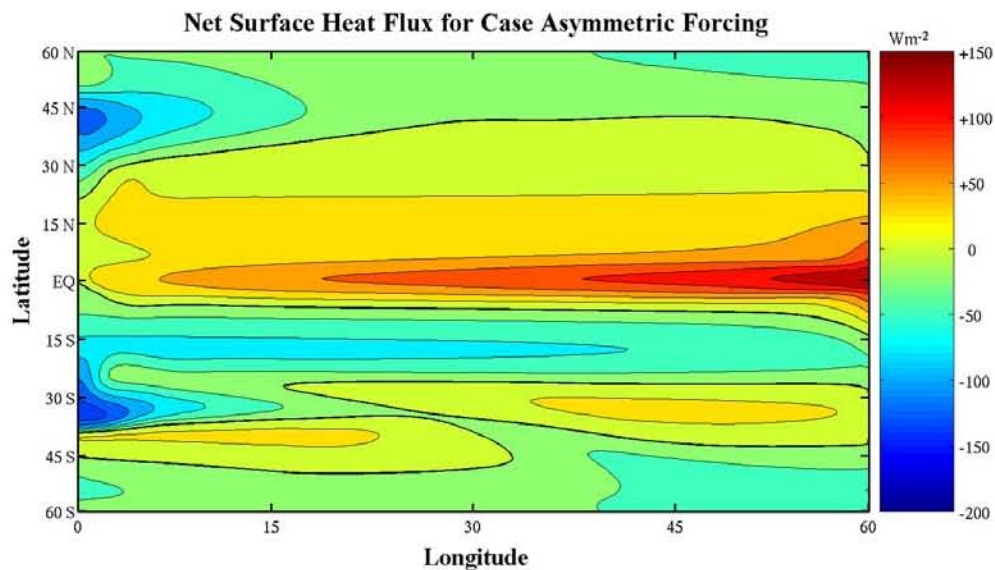


Figure 31. Net Surface Heat Flux for Symmetric Bathymetry and Asymmetric Forcing

## E. TWO-BASIN EXPERIMENT WITH SYMMETRIC BATHYMETRY AND FORCING

After inspection of the ACC path and its physical boundaries, it becomes apparent that there is a net northward displacement of the ACC as it enters the Atlantic through Drake's Passage and the flow returns south again as it rounds the Horn of Africa. Taking into account the fact that the ACC's southerly return is a shorter distance than the northerly excursion may indicate that some of the ACC's momentum is diverted to the maintenance of the Atlantic MOC. In order to investigate this hypothesis, a two-basin model was constructed with channel widths representing that of Drake's Passage and the passage between Antarctica and the southern tip of Africa (which is approximately three times the width of Drake's Passage). The Atlantic Ocean has the same symmetric bathymetry used in the previous models, and the Pacific Ocean is just a deep basin with a uniform depth of 4005 m. The two-basin bathymetry is shown in two and three dimensions in Figures 32 and 33. Symmetric wind and temperature forcing was applied and the model was exercised until equilibrium was reached. Output for the two-basin model run can be seen in Figures 34 and 35 in the form of sea surface temperature and net surface heat flux, respectively.

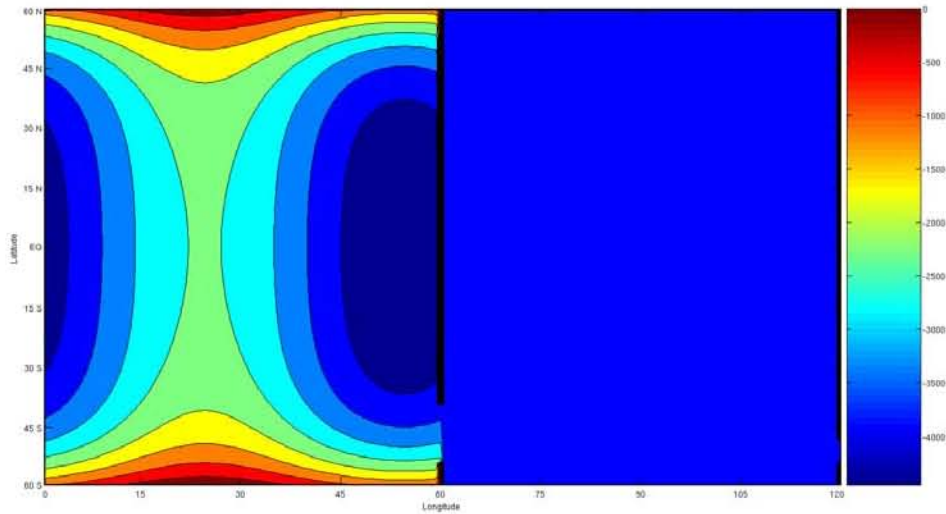


Figure 32. Two-dimensional Two-basin Bathymetry

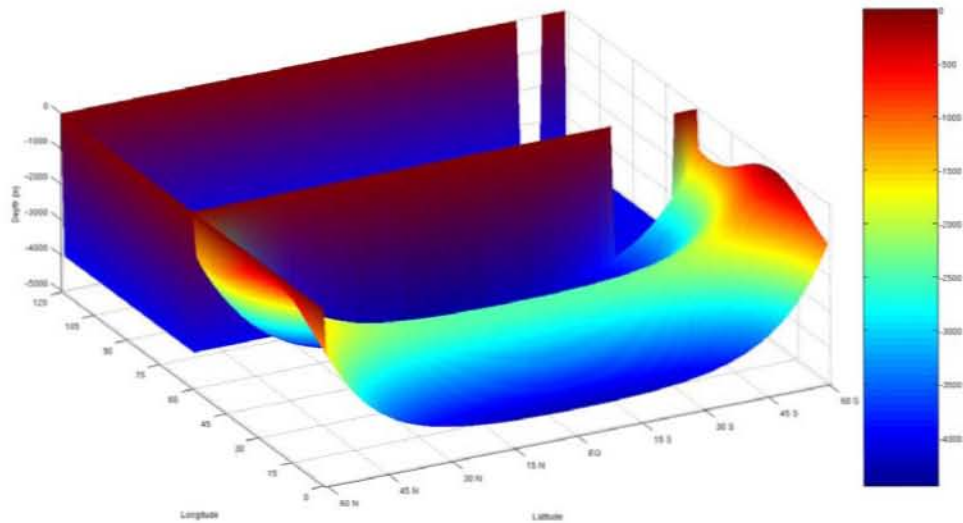


Figure 33. Three-dimensional Two-basin Bathymetry

This setup allows for easy comparison of results between basins with and without bathymetry. Of particular interest is the western portion of the Atlantic Basin. This region has slightly colder water in the mid-latitudes than the Pacific basin does due to the northward excursion of the ACC. The bathymetry also appears to draw colder water from the north into the mid-latitudes in the Atlantic Basin as well. The latter effect cannot be seen in the net surface heat flux, but the path of the ACC, however, is easily discernible in the Atlantic basin as the waters return poleward and heat is transferred from the surface of the ocean to the atmosphere.

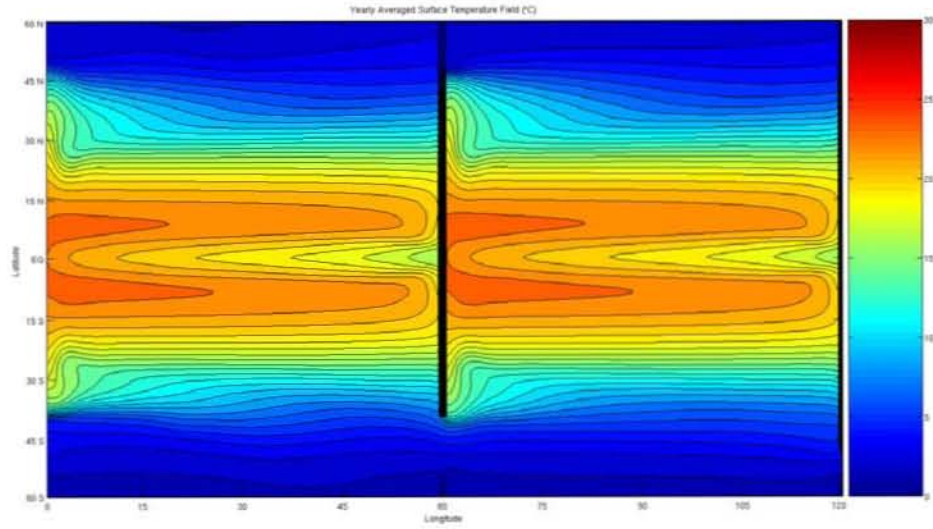


Figure 34. Sea Surface Temperature for Two Basins

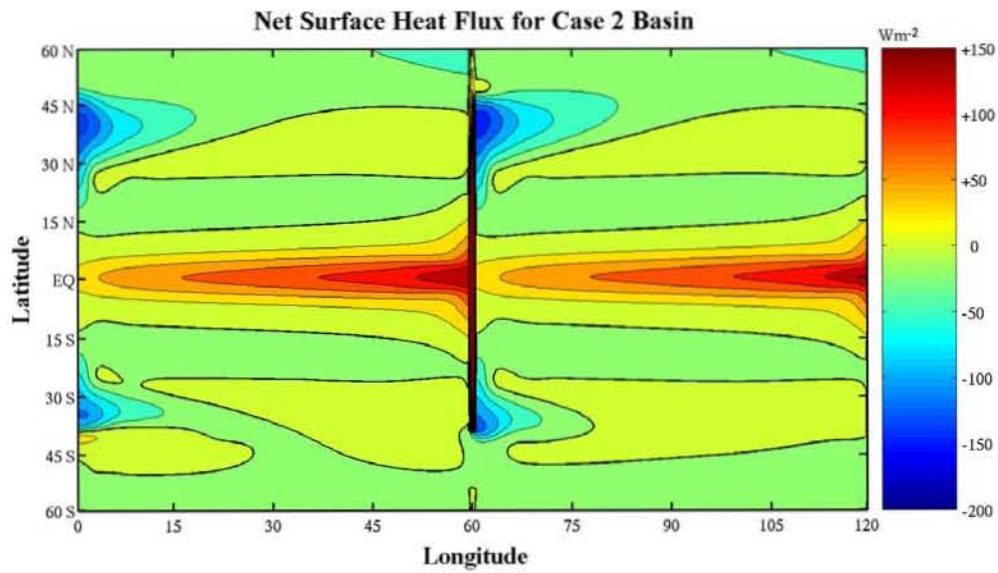


Figure 35. Net Surface Heat Flux for Two Basins

## IV. COMPARISON OF THE NUMERICAL EXPERIMENTS

### A. ELEMENTS OF THE DIAGNOSTIC MODEL

#### 1. Volume Transport

Measuring the volume transport in the meridional-vertical plane in the form of a volumetric streamfunction is perhaps the most logical method of defining the meridional overturning circulation. In order to do so, we start with the continuity equation:

$$\frac{\partial u}{\partial x} + \frac{\partial v}{\partial y} + \frac{\partial w}{\partial z} = 0. \quad (9)$$

Next, we integrate zonally, which results in:

$$\frac{\partial \mathbf{v}}{\partial y} + \frac{\partial \mathbf{w}}{\partial z} = 0 \quad (10)$$

where  $\mathbf{v} = \int_0^{L_x} v dx$  and  $\mathbf{w} = \int_0^{L_x} w dx$ .

Equation (10) can then be expressed as a streamfunction since the flow in the meridional-vertical plane is two-dimensional and non-divergent:

$$\mathbf{v} = \frac{\partial \Psi}{\partial z} \quad (11)$$

and

$$\mathbf{w} = -\frac{\partial \Psi}{\partial y}. \quad (12)$$

Using equation (11), the meridional volume transport is calculated by:

$$\Psi(\mathbf{y}, \mathbf{z}) = \int_{-H}^z \mathbf{v} dz \quad (13)$$

where  $\mathbf{v}$  is the time-averaged, zonally-integrated meridional velocity for a given depth and latitude. Since inter-hemispheric volume transport is the subject of interest for this research, only the volume transport at the equator is of importance and is given by:

$$\Psi_{Eq} = \max\left(\Psi|_{y=0}\right) \quad (14)$$

## 2. Heat Transport

Just as the streamfunction can be conveniently used to infer the inter-hemispheric volume transport, the “heatfunction” (Boccaletti et al. 2005) can be used to analyze the advective inter-hemispheric heat transfer. Starting with the advective-diffusion equation for temperature:

$$\frac{\partial T}{\partial t} + \frac{\partial(uT)}{\partial x} + \frac{\partial(vT)}{\partial y} + \frac{\partial(wT)}{\partial z} = K_H \nabla_H^2 T + K_V \frac{\partial^2 T}{\partial z^2} \quad (15)$$

and by neglecting interior diffusion in the central thermocline and applying time-averaging and zonal-integration Equation (15) yields:

$$\frac{\partial H_y}{\partial y} + \frac{\partial H_z}{\partial z} = 0, \quad (16)$$

where  $H_y = \int_0^{L_x} vT dx$  and  $H_z = \int_0^{L_x} wT dx$ .

Due to the lack of internal heat sources and heat sinks in the interior of the thermocline at steady-state, Equation (16) can be represented in the form of a “heatfunction”:

$$H_y = \frac{\partial \Psi_Q}{\partial z} \quad (17)$$

and

$$H_z = -\frac{\partial \Psi_Q}{\partial y}. \quad (18)$$

Heat transport can then be calculated in the meridional-vertical plane by taking into account the density of sea water and its heat capacity by and substituting them into Equation (17), giving:

$$\Psi_Q = c_p \rho \int_{-H}^z H_y dz \quad (19)$$

where  $c_p = 3850 \text{ J/kg}^\circ\text{C}$ ,  $\rho = 1025 \text{ kg/m}^3$ , and  $H_y$  represents the yearly-averaged, zonally-integrated meridional velocity and temperature for a given depth and latitude. As was the case for the volumetric streamfunction, the heat transport across the equator is the region of interest for this study and is given by the equation:

$$\Psi_{Q_{Eq}} = \max\left(\Psi_{Q_{y=0}}\right) \quad (20)$$

## B. PATTERNS OF THE HEAT AND VOLUME TRANSPORT AS A FUNCTION OF FORCING AND GEOMETRY

### 1. Inter-hemispheric Volume Transport

The ability to display volumetric transport as a streamfunction results from the derivation of Equation (14), which stems from Equation (9). Figures 36 through 40 represent meridional volumetric transport for the five model runs. In all cases, positive values of transport signify a counter-clockwise flow while negative values of transport signify clockwise flow. The bold line indicates the zero flow contour.

These volumetric streamfunctions look fairly similar to those of Edwards (2008) except for the inclusion of the deep overturning cell in the higher northern latitudes. This deep overturning cell did not occur in any of the model runs in Edwards (2008), however, all five model runs in this study contain this cell. The only consistent difference between all model runs in this study and all model runs from Edwards (2008) is the ACC itself, suggesting that the ACC may be the catalyst for this deep overturning cell. This deep overturning cell was not only observed by Boccaletti et al. (2005), but was also located around one kilometer in depth, as seen in Figure 41.

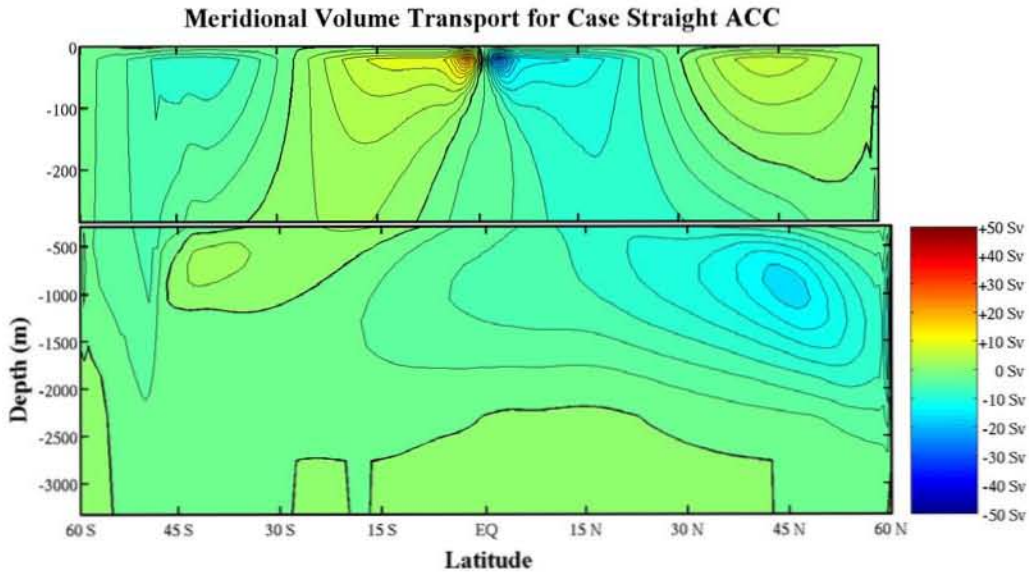


Figure 36. Inter-hemispheric Volume Transport for Idealized Basin with Antarctic Circumpolar Current



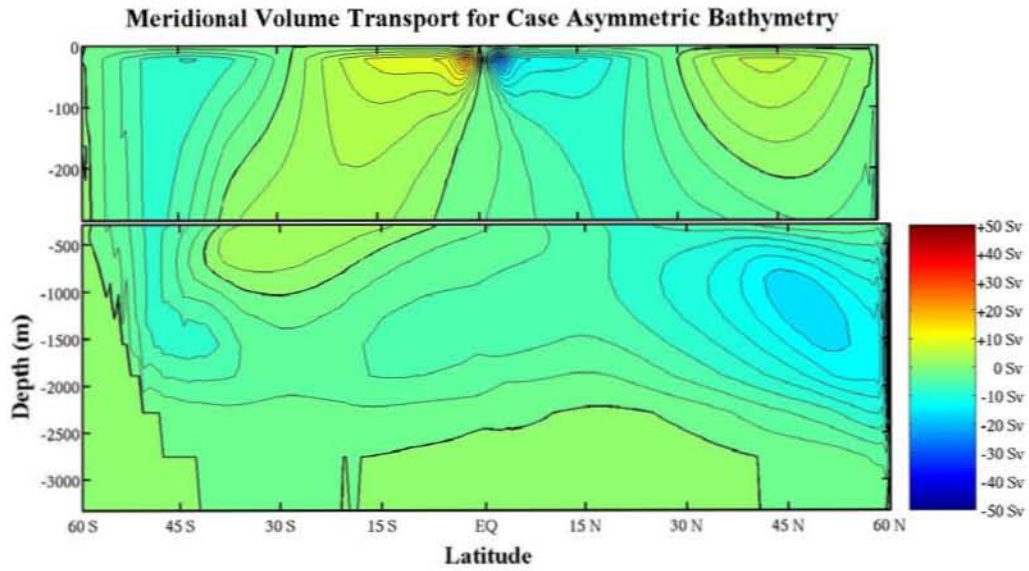


Figure 37. Inter-hemispheric Volume Transport for Asymmetric Bathymetry

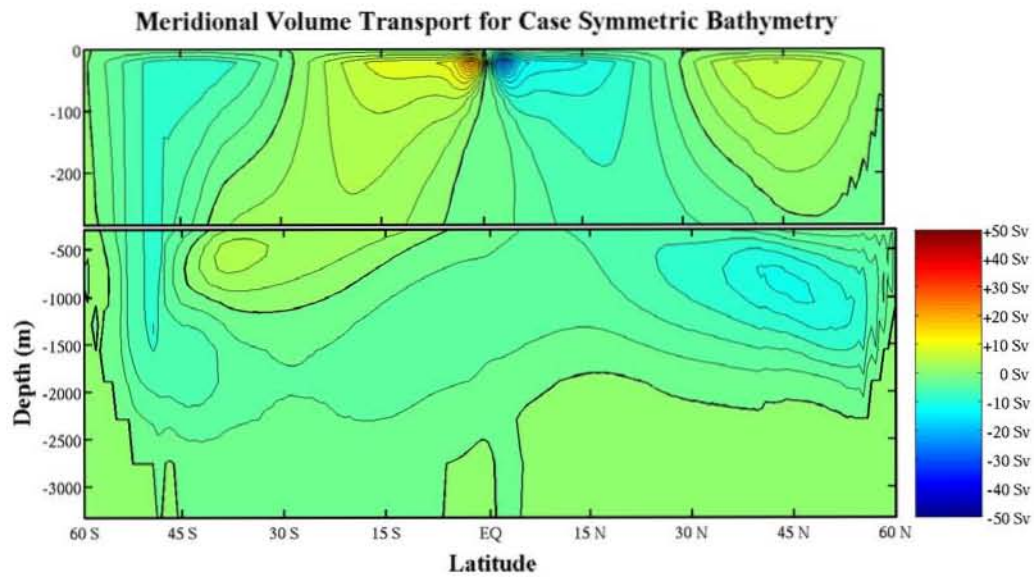


Figure 38. Inter-hemispheric Volume Transport for Symmetric Bathymetry



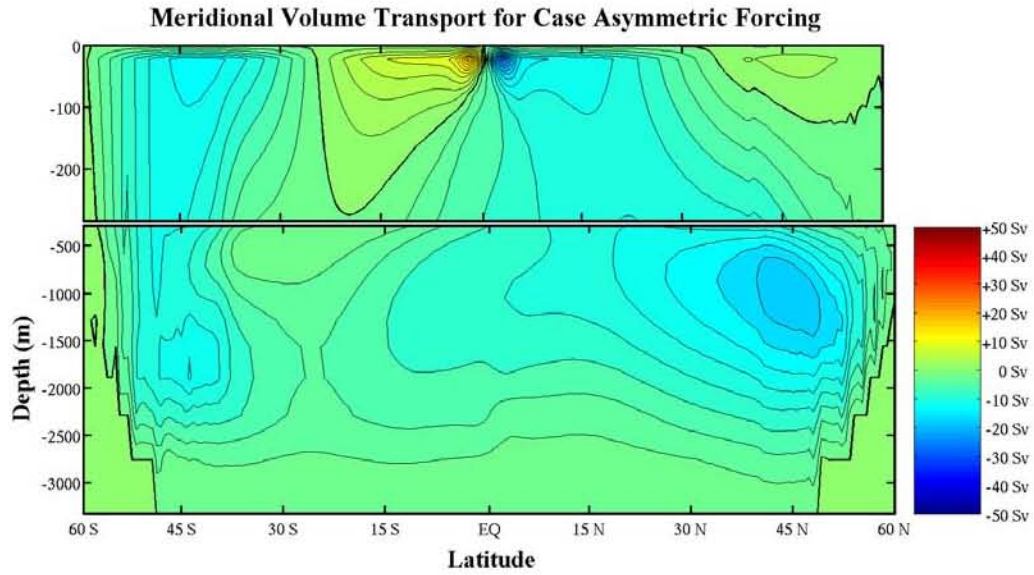


Figure 39. Inter-hemispheric Volume Transport for Symmetric Bathymetry and Asymmetric Forcing

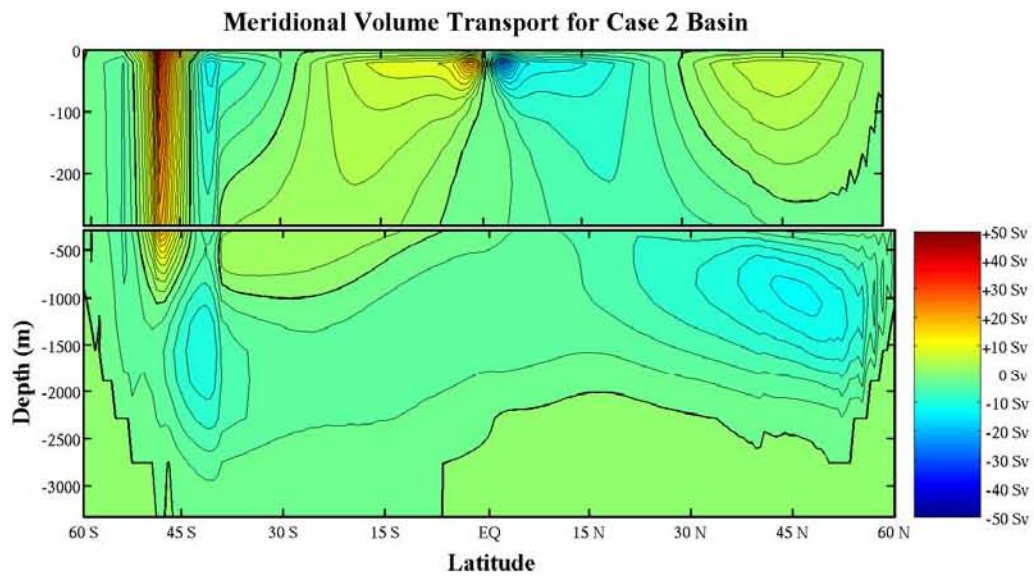


Figure 40. Inter-hemispheric Volume Transport for Two Basins

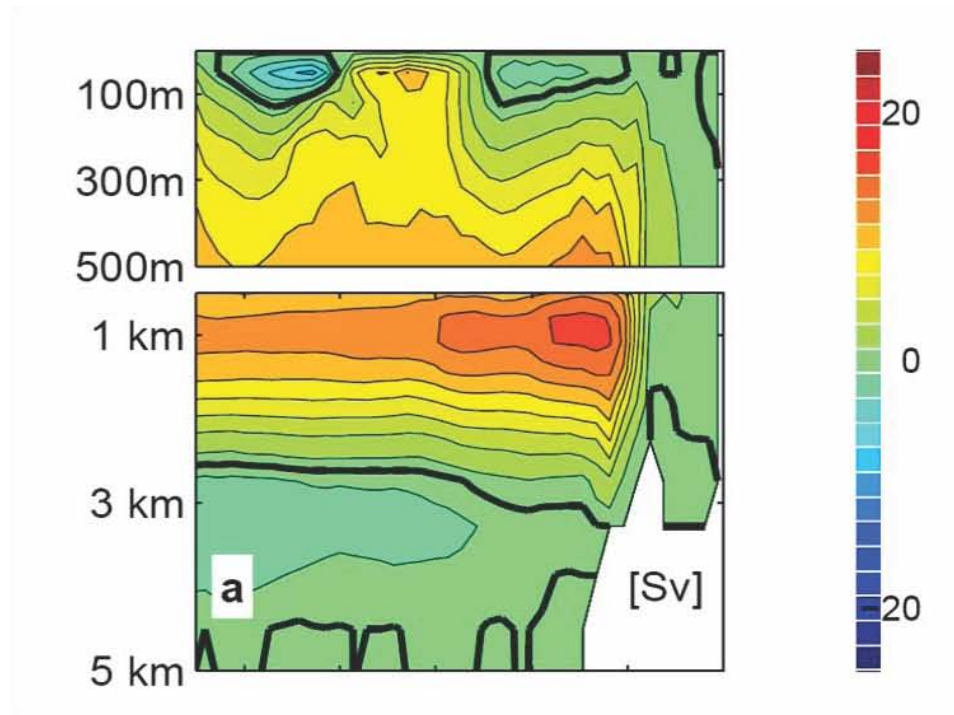


Figure 41. Deep Abyssal Overturning Cell (from Boccaletti et al., 2005)

## 2. Inter-hemispheric Heat Transport

The theoretical model leading to Equation (20) allows the use of a streamfunction showing the direction heat transport. The heat transport streamfunction, also known as a ‘heatfunction,’ for all five model runs in this study or shown in Figures 42 through 46. Positive values of heat transport signify counter-clockwise flow and negative values signify clockwise flow. The bold line denotes the zero flow contour. All five model runs appear to have fairly similar heatfunctions, but there were higher magnitudes of heat transport observed in the two-basin model run (Figure 46).

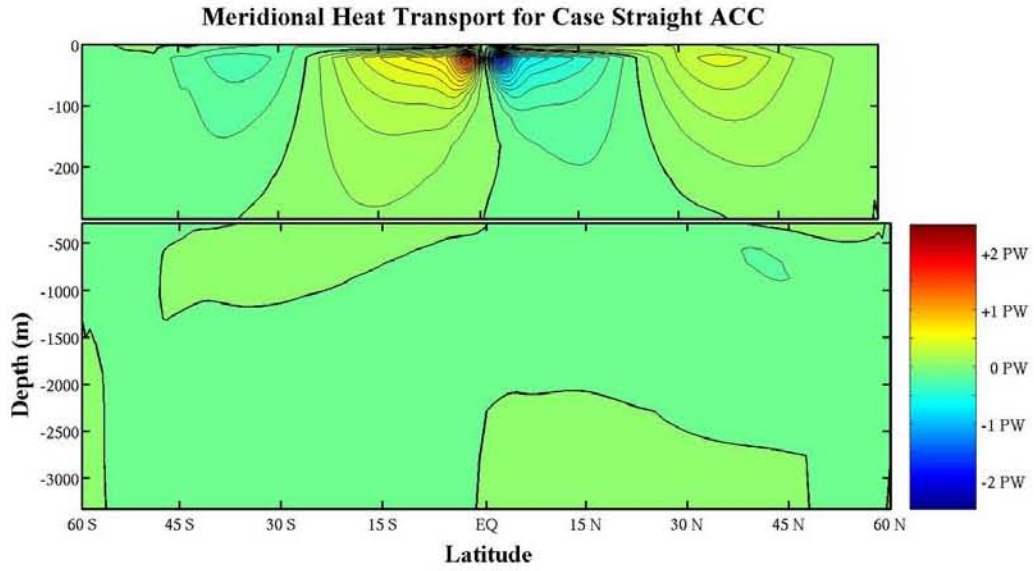


Figure 42. Heatfunction for the Straight ACC Model Run

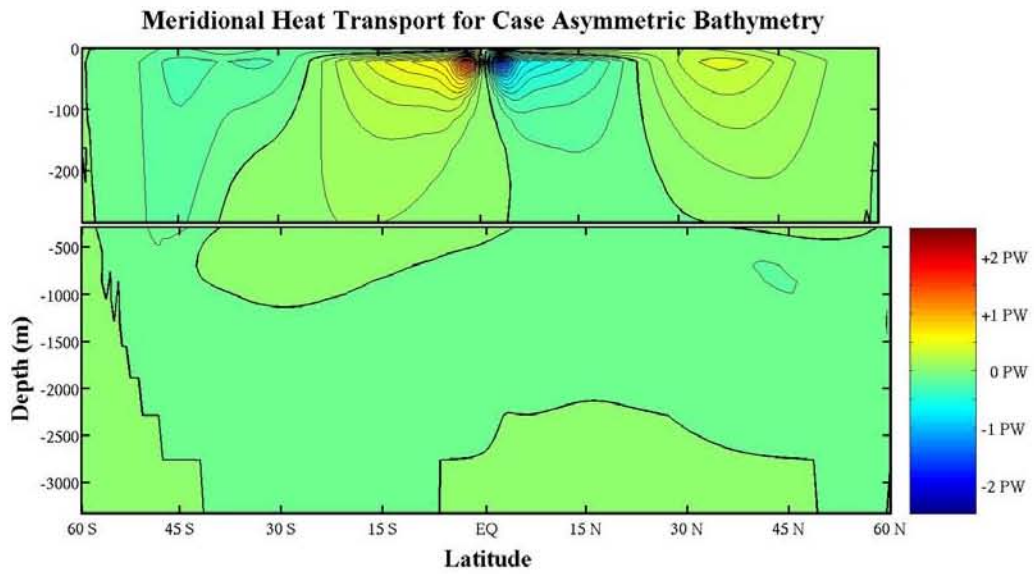


Figure 43. Heatfunction for the Asymmetric Bathymetry Model Run

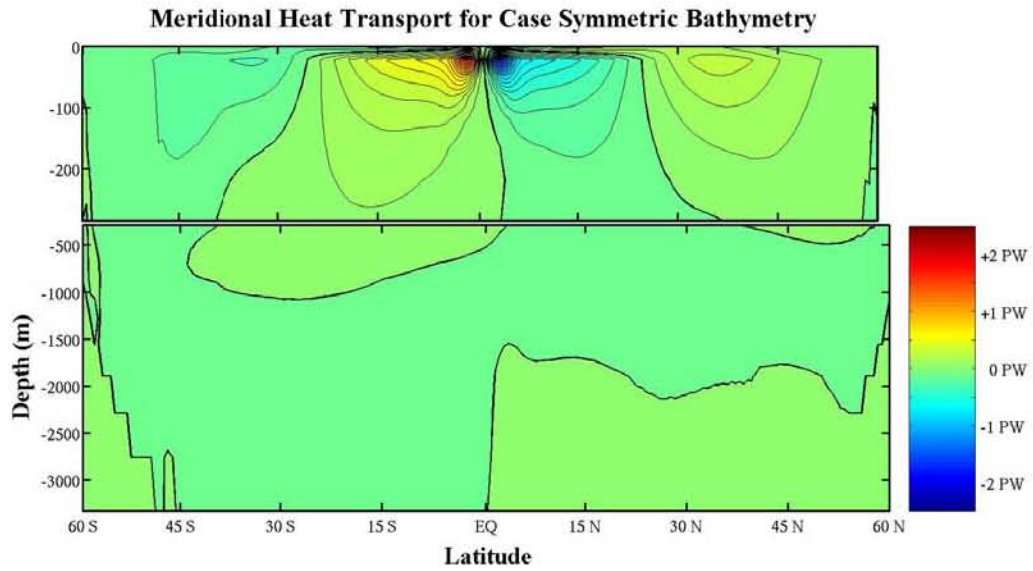


Figure 44. Heatfunction for the Symmetric Bathymetry Model Run

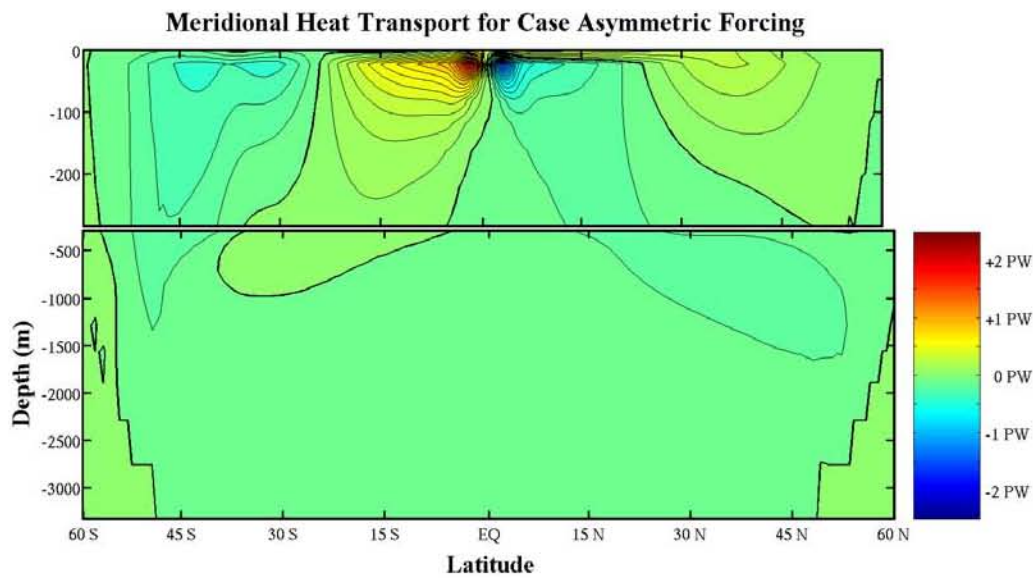


Figure 45. Heatfunction for the Symmetric Bathymetry with Asymmetric Forcing Model Run

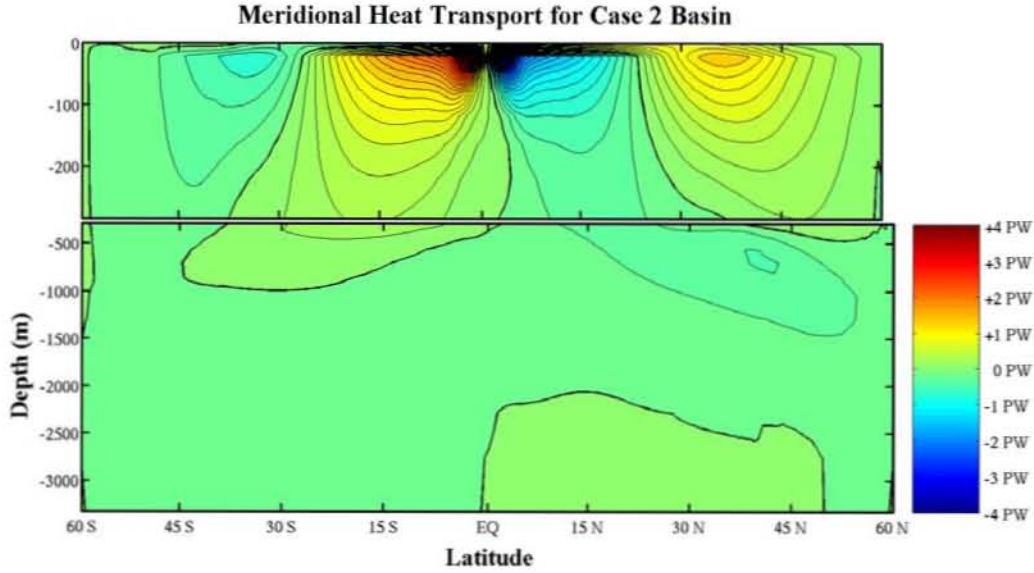


Figure 46. Heatfunction for the Two Basin Model Run

### C. MAGNITUDE OF THE INTER-HEMISPHERIC TRANSPORT AS A FUNCTION OF FORCING AND GEOMETRY

All pertinent results have been consolidated in Table 1. The first column denotes the run parameters. The second and third columns are the volumetric transport of the model MOC and the percentage of actual MOC, respectively. Likewise, the fourth and fifth columns are the model inter-hemispheric heat transport and the percentage of actual inter-hemispheric heat transport, respectively. The final row is the actual values of the respective parameters in each column for the Atlantic Ocean. The first two rows are model runs from Edwards (2008) with a basin geometry identical to that of the Straight ACC run before the addition of the ACC. These two runs have been added as a basis for comparison in order to determine the affect of the ACC on meridional circulation.

The first run in Table 1 is, in every aspect, symmetric about the equator and results in no inter-hemispheric transport. The second run is the same deep basin without an ACC with the application of asymmetric wind and temperature forcing. The asymmetry between the two hemispheres drives a net northward transport across the equator.

| <b>RUN</b>                                | <b>MOC (Sv)</b>        | <b>% OF ACTUAL</b> | <b>HEAT<br/>TRANSPORT<br/>(TW)</b> | <b>% OF ACTUAL</b> |
|---|------------------------|--------------------|------------------------------------|--------------------|
| Flat Bottom /<br>Sym Forcing / No<br>ACC  | 0                      | -                  | 0                                  | -                  |
| Flat Bottom /<br>Asym Forcing /<br>No ACC | 3.5                    | 19.4               | 225                                | 70.3               |
| Straight ACC                              | 3.3                    | 18.3               | 166.3                              | 52.0               |
| Asym Bathymetry                           | 4.0                    | 22.2               | 95                                 | 29.7               |
| Sym Bathymetry                            | 2                      | 11.1               | 70                                 | 21.9               |
| Sym Bathymetry<br>/ Asym Forcing          | 2.7                    | 15.0               | 400                                | 125.0              |
| 2-Basin                                   | 2.9 (Atl)<br>6.0 (Tot) | 16.1               | 143.9 (Atl)<br>341.9 (Tot)         | 45.0               |
| ACTUAL                                    | 18                     | ---                | 320                                | ---                |

Table 1. Model Run Results

The third run in Table 1 is the ideal basin from the first two runs with symmetric forcing and the inclusion of a representative ACC. The addition of the ACC leads to 3.3 Sv of MOC and 166.3 TW of inter-hemispheric heat transport. Comparison to the second run, which does not include the ACC, suggests that the ACC and surface forcing have equal impact upon MOC and inter-hemispheric heat transport.

The fourth and fifth model runs from Table 1 suggest that bathymetry has a fairly large effect on the amount of MOC and inter-hemispheric transport. Asymmetric bathymetry actually increased MOC while the addition of symmetric bathymetry reduced MOC by one half. In both cases, bathymetry reduced the amount of inter-hemispheric heat transport.

The sixth run in Table 1 combines symmetric bathymetry with asymmetric wind and temperature forcing. This configuration resulted in inter-hemispheric heat transports that are quite comparable to actual values. The asymmetric forcing also provided another four percent of MOC over the previous model configuration.



The final run in Table 1 is the two-basin setup described earlier with symmetric forcing. Comparison of this setup with the symmetric bathymetry and forcing run suggests that the return of the ACC to the latitude of Drake's Passage, when it occurs over multiple ocean basins, promotes a stronger MOC and greater inter-hemispheric transport. In this situation, the values of MOC increased another fifty percent and inter-hemispheric transport doubled over their respective values in the symmetric bathymetry model run.

It is important to note that the model results are misleading because the emphasis was placed on the thermocline layer with no attempt to adequately represent the abyssal layer. The actual values given in Table 1 take the entire ocean into account and have large error bars themselves.

Plots of meridional heat transport for each of the five model runs that comprise this study are shown in Figures 47 through 51. The plotted curves represent the zonally- and vertically-integrated heat transport at that given latitude. Positive values indicate northward heat transport at that location and negative values indicate southward heat transport at that location. In all five model runs in which the ACC was present, there is positive (northward) meridional transport at the equator.

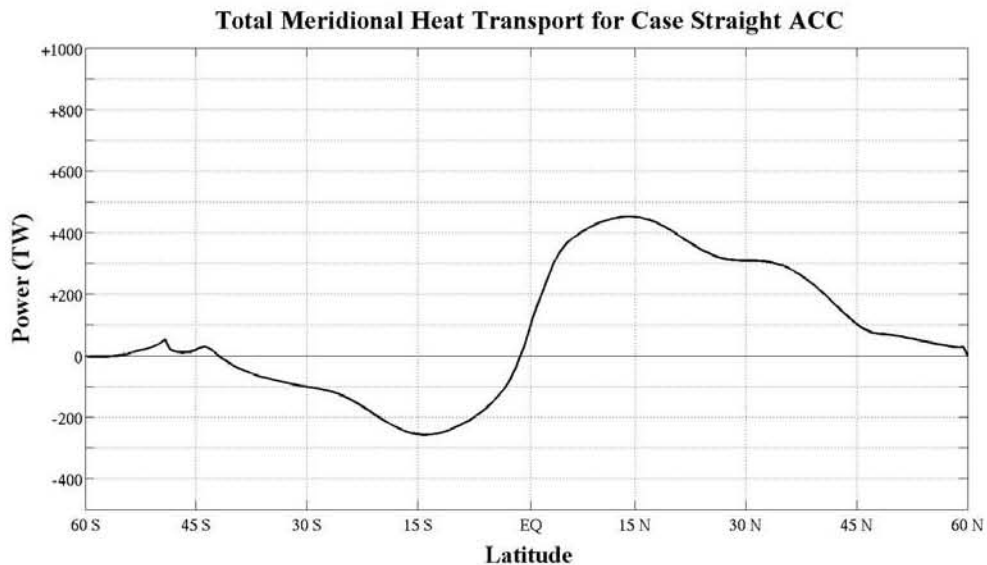


Figure 47. Total Heat Transport for Idealized Basin with Antarctic Circumpolar Current

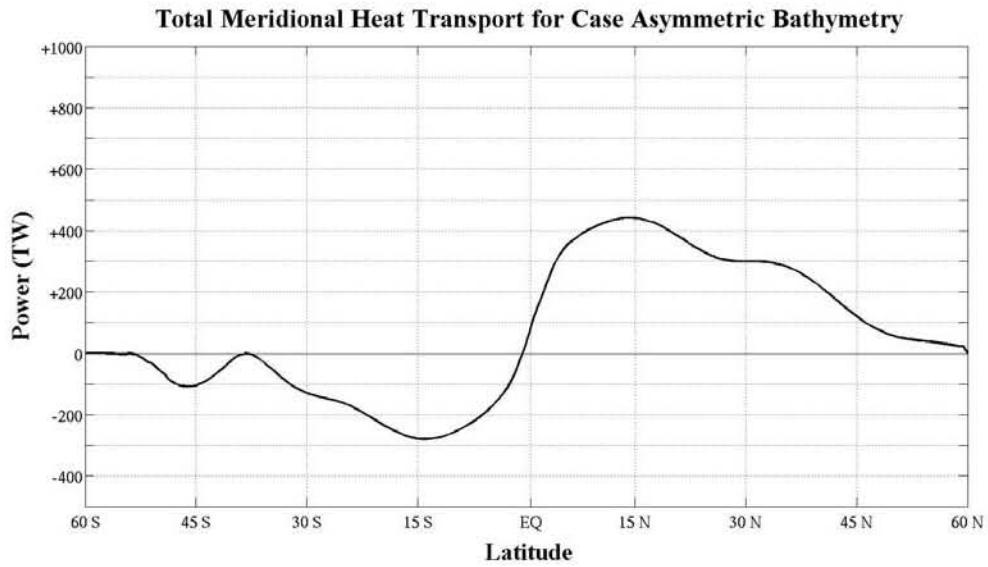


Figure 48. Total Heat Transport for Asymmetric Bathymetry

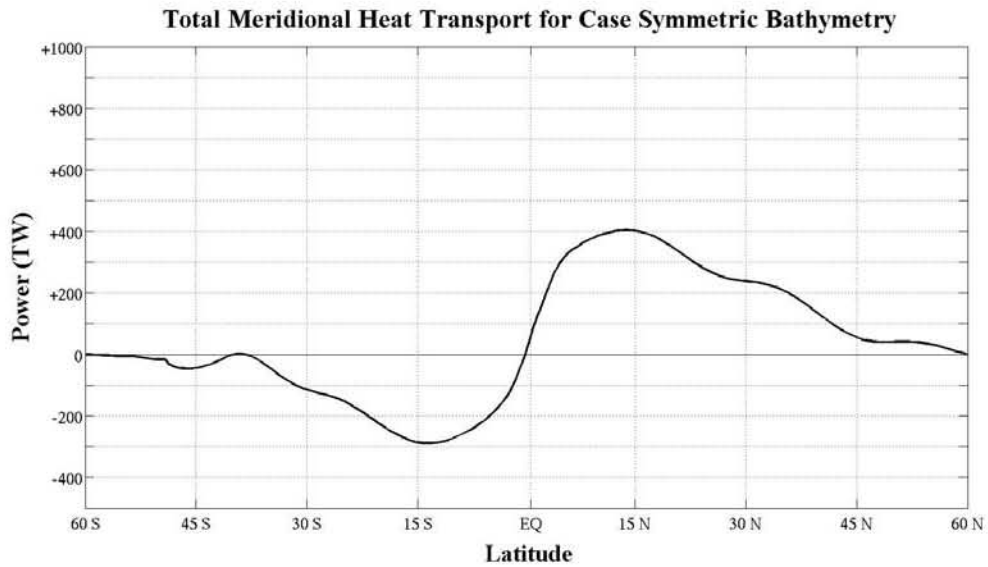


Figure 49. Total Heat Transport for Symmetric Bathymetry



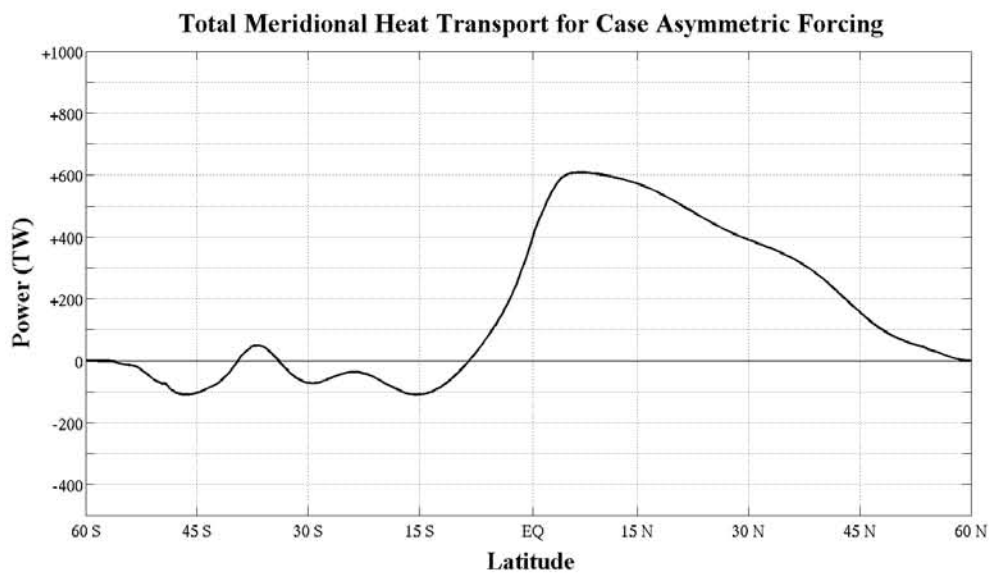


Figure 50. Total Heat Transport for Symmetric Bathymetry and Asymmetric Forcing

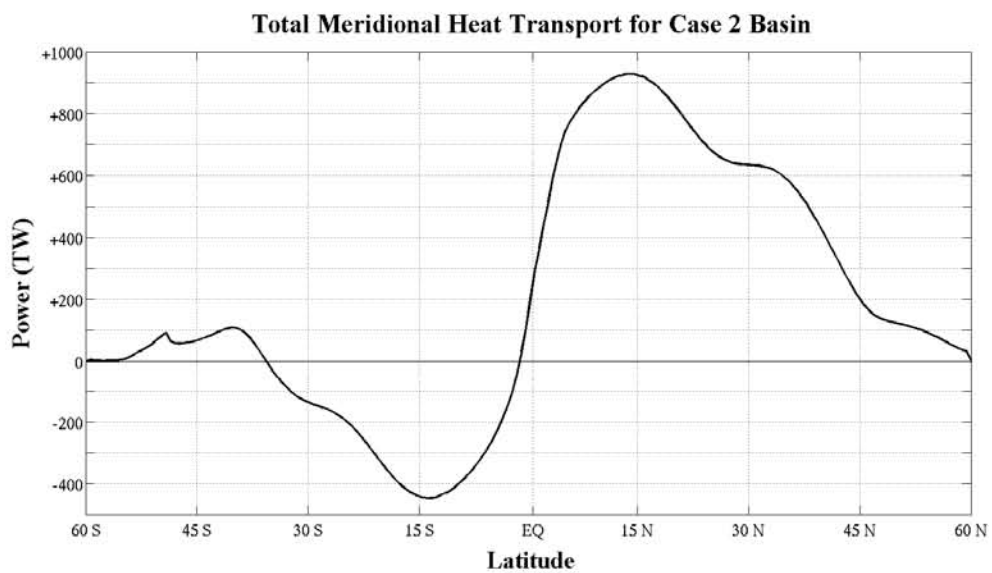


Figure 51. Total Heat Transport for Two Basins

THIS PAGE INTENTIONALLY LEFT BLANK

## V. DISCUSSION AND CONCLUSIONS

This study attempts to explain the dynamics of the inter-hemispheric transport of volume and heat. Of particular concern is the remote influence of the ACC. Our analysis is based on the intercomparison of circulation patterns observed in a series of numerical experiments in which we systematically vary the surface forcing and basin geometry.

An abyssal overturning cell was observed in all model runs that contained a representative ACC and was not observed in any of the idealized basin model runs of Edwards (2008). None of the model runs in Edwards (2008) attempted to simulate the ACC, suggesting that the ACC may be responsible for the creation and maintenance of the abyssal overturning cell in the higher, northern latitudes.

Comparison of runs using asymmetric forcing without the ACC and symmetric forcing with the ACC suggests that the Antarctic Circumpolar Current and asymmetric wind and temperature forcing have a nearly equal impact upon meridional circulation and inter-hemispheric heat transport, with each effect contributing approximately 19% of the MOC and 60% of inter-hemispheric heat transport.

The addition of asymmetric bathymetry effectively reduced the volumetric transport of the ACC with little impact on the MOC and a small reduction in inter-hemispheric heat transport. Taking the issue of bathymetry one step further, symmetric bathymetry significantly reduced the volume transport of the MOC with little effect on heat transport.

Combining asymmetric forcing along with the contribution of the ACC provided a slightly stronger MOC and a value of inter-hemispheric heat transport that is comparable to the actual amount of transport found in the Atlantic Ocean. The relatively large difference between the symmetric bathymetry and asymmetric bathymetry leads to the assumption that topography may also have a substantial impact on the MOC in the Atlantic Ocean.

The two-basin model, when compared to the run with symmetric bathymetry and forcing, provides very interesting insight into the effect of the ACC on MOC. The fact that MOC increased by a modest amount and inter-hemispheric heat transport doubled supports the hypothesis that the inter-hemispheric exchange flows are affected by the northerly excursion of the ACC as it leaves Drake's Passage and the shorter return to the southern tip of Africa. This conclusion can be drawn because the only difference in the Atlantic basin between the two runs is the width of the eastern channel; forcing and bathymetry is symmetric about the equator in both cases.

In summary, the meridional overturning circulation in the Atlantic Ocean indeed appears to be driven by asymmetries between the northern and southern hemispheres. The Antarctic Circumpolar Current is one of the most obvious asymmetries. As noted in previous research, it was found that topographic steering is essential to obtain an ACC with realistic volumetric flowrates and that in doing so, however, does not have much of an effect on inter-hemispheric heat and volume transports. Through comparison to model runs without an ACC, the ACC alone accounts for approximately 15% of the MOC and 60% of inter-hemispheric heat transport. Combining the ACC and asymmetries in forcing yields values that are quite similar to actual values, even in a highly idealized basin with such crude representative bathymetry.

## **VI. FUTURE RESEARCH**

The analysis presented in this study suggests that the theory of MOC would benefit from clarification of the following aspects:

### **A. EFFECTS OF THE RESOLVED EDDIES**

A relatively large effect on MOC and inter-hemispheric heat transport was observed in the model run containing the straight ACC. As mentioned earlier in the paper, it is possible that eddies are responsible for this meridional circulation and, therefore, a model that resolves eddies instead of parameterizing them may deem quite beneficial.

### **B. EFFECTS OF SALINITY**

Past research has proven that differences in water mass properties can drive a circulation. Even though the effect of the conventional thermohaline mechanisms on the MOC has been questioned, it is an integral component of the driving forces. An inclusion of the salinity effects, combined with the ACC and asymmetric wind and temperature forcing, and followed by detailed analysis of their interaction may be a critical ingredient required to give the ‘full picture’ of thermohaline circulation.

### **C. REALISTIC FORCING**

Wind and temperature forcing in all of the model runs was zonally uniform. Obviously this is not the case in reality. Seasonal variability in forcing may moderate the inter-hemispheric transports and result in more realistic values.

### **D. GLOBAL MODEL**

The two-basin model resulted in higher MOC and inter-hemispheric transport simply because the ACC did not have to return to the same latitude as Drake’s Passage at the eastern wall of the representative Atlantic Ocean basin. Small details such as this can often have large and unforeseen impacts. Ideally, a global model using polar coordinates with realistic bathymetry, climatology, and ocean water mass properties would provide

all of the pieces of the puzzle known as the Meridional Overturning Circulation. The idealized simulations presented in this study established a method of inquiry on which future studies should base the diagnostic of comprehensive models.

## LIST OF REFERENCES

- Adcroft, A., et al. (2009): *MITgcm User Manual*. MIT Department of EAPS, Cambridge, MA.
- Boccaletti, G., R. Ferrari, A. Adcroft, D. Ferreira, and J. Marshall (2005): The vertical structure of ocean heat transport. *Geophys. Res. Lett.*, **32**, L10603.
- Edwards, E., (2008), Pattern and dynamics of the Meridional Overturning Circulation in the upper ocean. M.S. thesis, Naval Postgraduate School.
- Gent, P., and J. McWilliams (1995): Isopycnal mixing in ocean circulation models. *J. Phys. Oceanogr.*, **20**, 150-155.
- Gnanadesikan, A. (1999): A simple predictive model for the structure of the oceanic pycnocline. *Science*, **283**, 2077-2079.
- Kuhlbrodt, T., A. Griesel, M. Montoya, A. Levermann, M. Hofmann, and S. Rahmstorf (2004): On the driving processes of the Atlantic meridional overturning circulation. *Rev. Geophys.*, **45**, 2004RG000166.
- Marshall, J., and T. Radko (2003): Residual-mean solutions for the Antarctic Circumpolar Current and its associated overturning circulation. *J. Phys. Oceanogr.*, **33**, 2341-2354.
- Munk, W. H. (1966), Abyssal recipes. *Deep Sea Research*, **13**, 707-730.
- Munk, W. H., and E. Palmén (1951): Note on the dynamics of the Antarctic Circumpolar Current, *Tellus*, **3**, 53-55.
- Olbers, D., D. Borowski, C. Volker, and J. O. Wolff (2004): The dynamical balance, transport and circulation of the Antarctic Circumpolar Current, *Antarct. Sci.*, **16**, 439-470.
- Radko, T. (2007): A mechanism for establishment and maintenance of the meridional overturning in the upper ocean, *J. Mar. Res.*, **65**, 85-116.
- Robinson, A. R., and H. Stommel (1959): The oceanic thermocline and the associated thermohaline circulation, *Tellus*, **11**, 295-308.
- Timmermann, A., and H. Goosse (2004): Is the wind stress forcing essential for the meridional overturning circulation? *Geophys. Res. Lett.*, **31**, L04303.

- Toggweiler, J. R., and B. Samuels (1998): On the ocean's large-scale circulation near the limit of no vertical mixing, *J. Phys. Oceanogr.*, **28**, 1832-1852.
- Webb, D. J., and N. Suginohara (2001), Vertical mixing in the ocean, *Nature*, **409**, 37.
- Welander, P. (1986): Thermohaline effects in the ocean circulation and related simple models, *Large-Scale Transport Processes in Oceans and Atmosphere*, J. Willebrand and D. L. T. Anderson, Eds., D. Reidel, 163-200.
- Whitworth, T. III (1983): Monitoring the transport of the Antarctic Circumpolar Current at Drake's Passage, *J. Phys. Oceanogr.*, **13**, 2045-2057.
- Whitworth, T. III, and R. Peterson (1985): Volume transport of the Antarctic Circumpolar Current from bottom pressure measurements, *J. Phys. Oceanogr.*, **15**, 810-816.
- Wunsch, C., and R. Ferrari (2004): Vertical mixing, energy, and the general circulation of the oceans, *Annu. Rev. Fluid Mech.*, **36**, 281-314.
- Wyrski, K. (1961): The thermohaline circulation in relation to the general circulation in the oceans, *Deep Sea Research*, **8**, 39-64.



## INITIAL DISTRIBUTION LIST

1. Defense Technical Information Center  
Ft. Belvoir, Virginia
2. Dudley Knox Library  
Naval Postgraduate School  
Monterey, California
3. Timour Radko  
Department of Oceanography  
Naval Postgraduate School  
Monterey, California
4. Jeffrey Haferman  
Naval Postgraduate School  
Monterey, California
5. Jeff Paduan  
Department of Oceanography  
Naval Postgraduate School  
Monterey, California